NORSAR

ROYAL NORWEGIAN COUNCIL FOR SCIENTIFIC AND INDUSTRIAL RESEARCH

Scientific Report 1-78/79

FINAL TECHNICAL SUMMARY

1 April - 30 September 1978

D. Rieber-Mohn (ed.)

Kjeller, October 1978

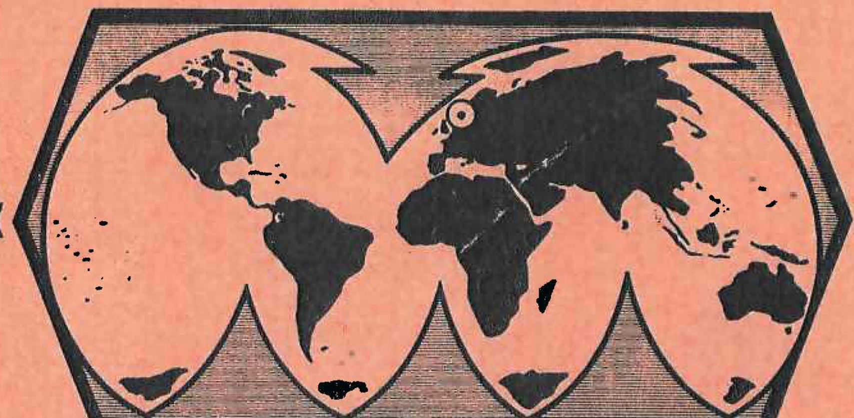

APPROVED FOR PUBLIC RELEASE, DISTRIBUTION UNLIMITED

SECURITY CLASSIFICATION OF THIS PAGE (When Data Entered)

REPORT DOCUMENTATION PAGE

READ INSTRUCTIONS BEFORE COMPLETING FORM

1. REPORT NUMBER F08606-78-C-0005	2. GOVT ACCESSION NO.
3. RECIPIENT'S CATALOG NUMBER	
4. TITLE (and Subtitle) Final Technical Summary	5. TYPE OF REPORT & PERIOD COVERED 1 April 78 - 31 September 78
	6. PERFORMING ORG. REPORT NUMBER Sci. Rep. No. 1-78/79
7. AUTHOR(s) D. Rieber-Mohn (Ed.)	8. CONTRACT OR GRANT NUMBER(s) F08606-78-C-0005
9. PERFORMING ORGANIZATION NAME AND ADDRESS NTNF/NORSAR P.O. Box 51, N-2007 Kjeller, Norway	10. PROGRAM ELEMENT, PROJECT, TASK AREA & WORK UNIT NUMBERS Norsar Phase 3
11. CONTROLLING OFFICE NAME AND ADDRESS	12. REPORT DATE 31 October 1978
	13. NUMBER OF PAGES 73
14. MONITORING AGENCY NAME & ADDRESS(if different from Controlling Office) VELA Seismological Center 312 Montgomery Street Alexandria, VA 22314 USA	15. SECURITY CLASS. (of this report)
	15a. DECLASSIFICATION/DOWNGRADING SCHEDULE

16. DISTRIBUTION STATEMENT (of this Report)

APPROVED FOR PUBLIC RELEASE; DISTRIBUTION UNLIMITED.

17. DISTRIBUTION STATEMENT (of the abstract entered in Block 20, if different from Report)

18. SUPPLEMENTARY NOTES

19. KEY WORDS (Continue on reverse side if necessary and identify by block number)

20. ABSTRACT (Continue on reverse side if necessary and identify by block number)

This report describes the operation and research activities at the Norwegian Seismic Array (NORSAR) for the time period from 1 April to 30 September 1978. In general, the array operation is characterized as stable, with little change from the previous reporting period. There has been a slight improvement in the performance of the data recording and online detection processing relative to the previous reporting period (uptime increased to 93.7% from 91.6%). The Special Processing System (SPS) is still the

DD FORM 1 JAN 73 1473 EDITION OF 1 NOV 65 IS OBSOLETE

SECURITY CLASSIFICATION OF THIS PAGE (When Data Entered) major cause of the breaks in operation (75 out of 139), the longest one lasting for more than 4 days. Statistics from short sample intervals indicate that the number of Online detections average about 200 per day with the present threshold setting, while the On-line Event Processor processes about 25 events per day for transmission to the SDAC. The average number of analyst-retrieved and accepted events has been 10.8 per day during the period.

The work load for the data center has been too large to handle within the regular working hours. Long jobs must be run during evenings, and additional part time help has been employed, in order to catch up with Data Retention processing outside working hours. NORSAR personnel have gradually taken over more responsibility for maintenance and error corrections of hardware (tape drives, SPS, etc.). The performance of the array's communications circuits has been satisfactory during the period, with three outages lasting for more than one hour and affecting more than one subarray simultaneously. One case of attenuation distortion has been discovered on the ARPANET SDAC communications circuit. No changes have been made to the TIP or its connections within the reporting period. There have been few modifications to the Online Detection Processor, the most important being implementation of logic to stop the system when erroneous timing is discovered, and a change in the selection of the channels that are automatically transmitted to SDAC with each processed event. An off-line interactive bulletin editing system has been implemented.

In the beginning of the reporting period, a Teledyne-Geotech S-500 seismometer was tested out within the array configuration (subarray 06C). It was removed on 12 April. Also, on 5 April, a Teledyne-Geotech S-13 three-axis seismometer was installed at subarray 01A. The components were connected to standard NORSAR channel equipment. The relatively large number of maintenance visits in this period (average 9.3 per subarray), is mainly due to preventive maintenance work such as painting, amplifier replacements and instrument adjustments.

The research work at NORSAR in the period is described in eight subsections in Chapter VI. They cover evaluation of the NORSAR Detection and Location capabilities and other research conducted under NTNF's contract with ARPA, as well as projects sponsored by Norwegian authorities. In the evaluation of detection capability in Section VI.1 it is found that the average monthly number of events reported in the edited NORSAR seismic bulletin now is reduced to about 60% of the level when 22 subarrays were in operation, or to 65% if one compensates for the increased system downtime. This corresponds to a reduction in the 50% incremental detectability threshold of about 0.2 m_b units, which agrees well with theoretical expectations. The event location capability of the present NORSAR array is evaluated in Section VI.2, and the median location difference between NORSAR and USGS epicentral solutions is found to be 230 km in the teleseismic distance range. Section VI.3 presents results on our continued seismic magnitude studies, in particular regarding the M_s:m_b relationship. Sections VI.4, VI.5 and VI.6 present initial results from a detection and discrimination study based upon near-field observations. The data base for these studies will be greatly expanded during the forthcoming year. A study of the general question of to what extent tectonic features observable at the surface have counterparts in the deeper parts of the lithosphere is presented in Section VI.7. Section VI.8 presents initial data analysis results from the Stiegler's Gorge Seismic Network installed by NTNF/NORSAR for the purpose of seismic risk studies in Tanzania. Finally, Section VI.9 presents results from the continued investigation of the seismicity of Svalbard.

AFTAC Project Authorization No.	:	VELA VT/8702/B/PMP
ARPA Order No.	:	2551
Program Code No.	:	8F10
Name of Contractor	:	Royal Norwegian Council for Scientific and Industrial Research
Effective Date of Contract	:	1 October 1977
Contract Expiration Date	:	30 September 1978
Contract No.	:	F08606-78-C-0005
Project Manager	:	Frode Ringdal (02) 71 69 15
Title of Work	:	The Norwegian Seismic Array (NORSAR) Phase 3
Amount of Contract	:	$520,000

This research was supported by the Advanced Research Projects Agency of the Department of Defense and was monitored by AFTAC, Patrick AFB FL 32925, under contract no. F08606-78-C-0005.

NORSAR Contribution No. 258

TABLE OF CONTENTS

I. SUMMARY

This report describes the operation and research activities at the Norwegian Seismic Array (NORSAR) for the time period from 1 April to 30 September 1978. In general, the array operation is characterized as stable, with little change from the previous reporting period. There has been a slight improvement in the performance of the data recording and online detection processing relative to the previous reporting period (uptime increased to 93.7% from 91.6%). The Special Processing System (SPS) is still the major cause of the breaks in operation (75 out of 139), the longest one lasting for more than 4 days. Statistics from short sample intervals indicate that the number of Online detections average about 200 per day with the present threshold setting, while the On-line Event Processor processes about 25 events per day for transmission to the SDAC. The average number of analyst-retrieved and accepted events has been 10.8 per day during the period.

The work load for the data center has been too large to handle within the regular working hours. Long jobs must be run during evenings, and additional part time help has been employed, in order to catch up with Data Retention processing outside working hours. NORSAR personnel have gradually taken over more responsibility for maintenance and error corrections of hardware (tape drives, SPS, etc.). The performance of the array's communications circuits has been satisfactory during the period, with three outages lasting for more than one hour and affecting more than one subarray simultaneously. One case of attenuation distortion has been discovered on the ARPANET SDAC communications circuit. No changes have been made to the TIP or its connections within the reporting period. There have been few modifications to the Online Detection Processor, the most important being implementation of logic to stop the system when erroneous timing is discovered, and a change in the selection of the channels that are automatically transmitted to SDAC with each processed event. An off-line interactive bulletin editing system has been implemented.

In the beginning of the reporting period, a Teledyne-Geotech S-500 seismometer was tested out within the array configuration (subarray 06C). It was removed on 12 April. Also, on 5 April, a Teledyne-Geotech S-13 three-axis seismometer was installed at subarray 01A. The components were connected

to standard NORSAR channel equipment. The relatively large number of maintenance visits in this period (average 9.3 per subarray), is mainly due to preventive maintenance work such as painting, amplifier replacements and instrument adjustments.

The research work at NORSAR in the period is described in eight subsections in Chapter VI. They cover evaluation of the NORSAR Detection and Location capabilities and other research conducted under NTNF's contract with ARPA, as well as projects sponsored by Norwegian authorities. In the evaluation of detection capability in Section VI.1 it is found that the average monthly number of events reported in the edited NORSAR seismic bulletin now is reduced to about 60% of the level when 22 subarrays were in operation, or to 65% if one compensates for the increased system downtime. This corresponds to a reduction in the 50% incremental detectability threshold of about 0.2 m_b units, which agrees well with theoretical expectations. The event location capability of the present NORSAR array is evaluated in Section VI.2, and the median location difference between NORSAR and USGS epicentral solutions is found to be 230 km in the teleseismic distance range. Section VI.3 presents results on our continued seismic magnitude studies, in particular regarding the M_s:m_b relationship. Sections VI.4, VI.5 and VI.6 present initial results from a detection and discrimination study based upon near-field observations. The data base for these studies will be greatly expanded during the forthcoming year. A study of the general question of to what extent tectonic features observable at the surface have counterparts in the deeper parts of the lithosphere is presented in Section VI.7. Section VI.8 presents initial data analysis results from the Stiegler's Gorge Seismic Network installed by NTNF/NORSAR for the purpose of seismic risk studies in Tanzania. Finally, Section VI.9 presents results from the continued investigation of the seismicity of Svalbard.

II. OPERATION OF ALL SYSTEMS

II.1 Detection Processor (DP) Operation

There have been 139 breaks in the otherwise continuous operation of the NORSAR Online DP system within the current 6-month reporting interval. The uptime percentage is 93.7%, which is a slight improvement over the 91.6% reported for the previous interval (October 77-March 78). Fig. II.1.1 and the accompanying Table II.1.1 both show the daily DP downtime for the days between 1 April and 30 September 1978. The monthly recording times and up percentages are given in Table II.1.2. As can be seen from Table II.1.1, the longest break occurred from mid-day 18 May to mid-day 22 May and lasted more than 96 hours. A power break brought the SPS down and acted as a catalyst to bring forward an inherent SPS hardware error, which subsequently was found and corrected. In addition, the stops related to the SPS alone were 75, so that obviously this component maintains its status as the weakest link in the system. The breaks can be grouped as follows:

a)	SPS malfunctioning	:	75
b)	Error on the Multiplexor Channel	:	16
c)	Stops related to possible program errors	:	12
d)	Maintenance stops	:	12
e)	Power jumps and breaks	:	10
f)	Hardware problems	:	5
g)	Magnetic tape drive problems	:	4
h)	Stops related to system operation	:	3
i)	TOD error stops	:	2

The varying performance of the SPS is reflected in the fact that the stops caused by this component occur in 'bursts', with long quiet periods in between, when the SPS performs normally. (See also comments elsewhere in this report.)

The number of stops caused by the error on the multiplexor channel (category b) is exactly twice the corresponding number for the last reporting period. However, as can be seen from Table II.1.1, 12 of the 16 stops in this category occurred within daily working hours, so that the system was restarted promptly. The probable cause of this type of error is the use of the printer, which seems to put a too heavy load on the multiplexor channel. Neither the printer nor the operator console are used, however, outside working hours.

The relatively high number of program errors reflects partly the strain on the 360-based Online system when the SPS is behaving abnormally. Any such situation causing all the available queue storage to be used will, for instance, show itself as a program error in the queue block leasing routine. The continuous effort of NORSAR personnel to maintain a system with optimum performance is reflected in the number of maintenance stops (category d), which shows an increase from last reporting period. This is partly caused by the more intensive care necessary for the SPS subsystem.

The total downtime for this period was 274 hours 51 minutes. The mean-time-between-failures (MTBF) was 1.2 days, as compared with 1.5 days for the previous reporting period.

The average Detection Rates (number of detections per day) for the NORSAR Online System's Detection task, and the average Event Rates (number of events per day) for the Online Event Processor (OEP) subtask in the same system are given in Table II.1.3. For practical reasons, we have not been able to provide comprehensive statistics during this reporting period; instead we present the data for short time intervals in the beginning, middle and end of the period. The cases of Coherent and Incoherent Detection/Event processing have been separated. As can be seen, the Event Rates are significantly less than the corresponding Detection Rates. This is to be expected, since the OEP has somewhat higher signal-to-noise ratio thresholds for its event candidates than the corresponding detection thresholds (3.6 and 2.4 versus 3.16 and 1.6, respectively). This difference is sufficient to eliminate most of the noise detections from consideration. The table also seems to indicate that the total number of OEP events is relatively constant and independent of the Detection Rates (about 24 events per day). However, insufficient statistics prevent any firm conclusions to be drawn, even when, as in this case, the sampled intervals are spread out in time. As an example of the variability of daily Detection and Event Rates, Fig. II.1.2 shows these parameters for (A) a 5-day interval in July and (B) for a 5-day interval in September.

D. Rieber-Mohn

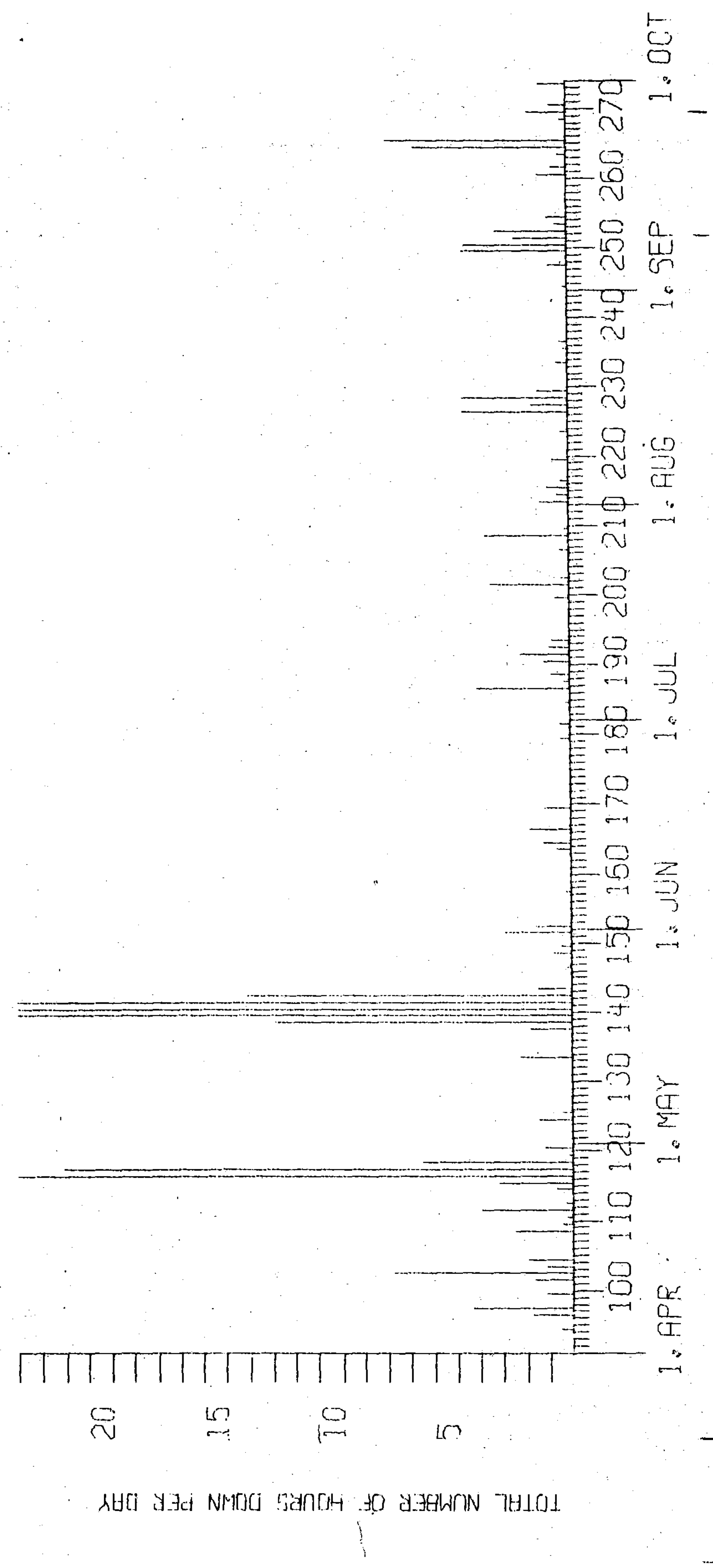

Fig. II.1.1   Online System Downtime, April - September 1978

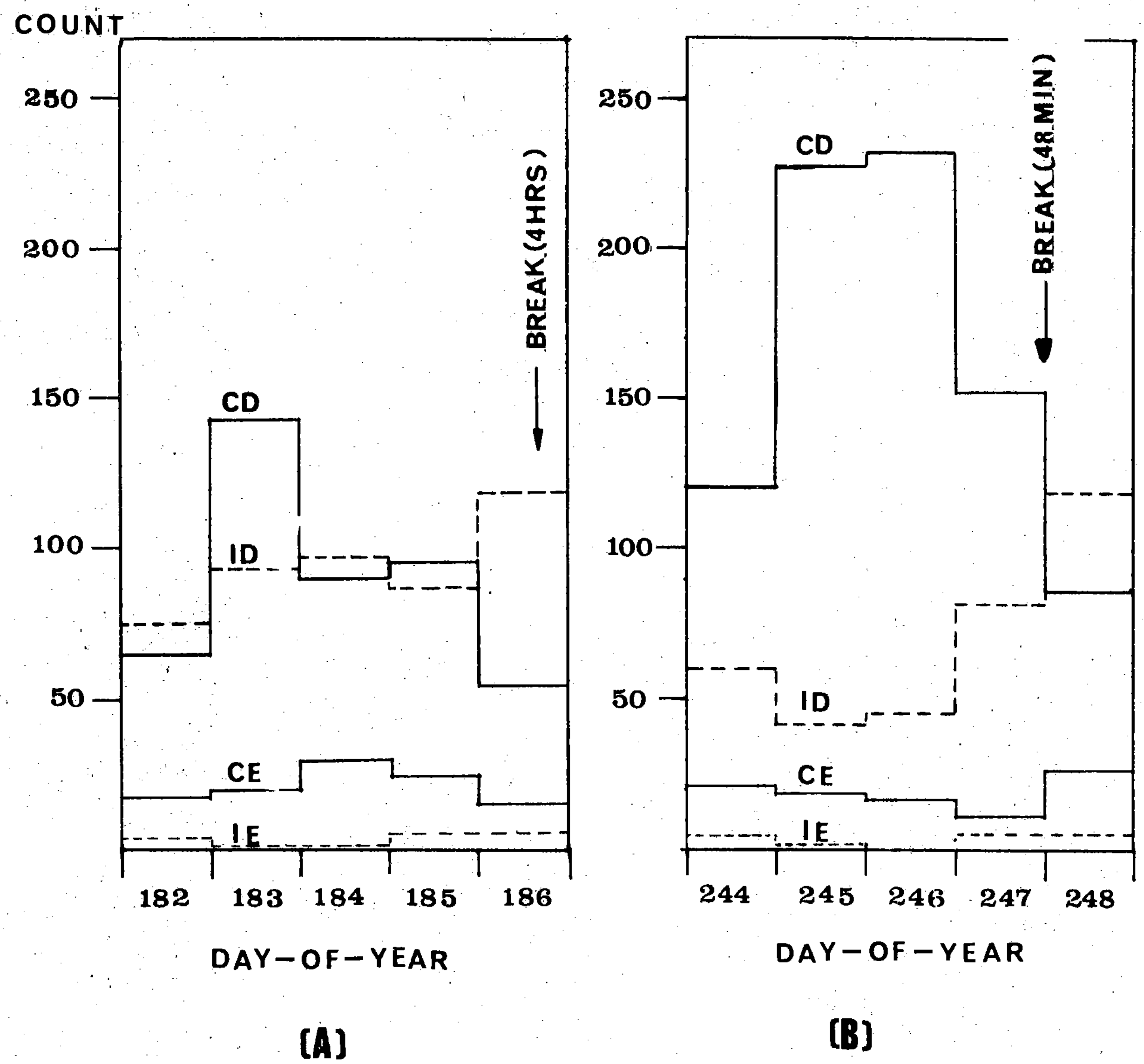

Fig. II.1.2 Variability in the coherent and incoherent detection and event rates. (A) 5 days in July; (B) 5 days in September.

CD: Coherent Detections
CE: Coherent Events
ID: Incoherent Detections
IE: Incoherent Events.

LIST OF BREAKS IN DP PROCESSING THE LAST HALF-YEAR

DAY	START		STOP		COMMENTS...........
94	11	53	11	57	ERRONEOUS SPS TIMING
94	15	20	15	46	SPS STOP
96	9	36	10	0	SPS NO DETECTIONS
96	11	44	12	6	ERRONEOUS SPS TIMING
96	15	40	16	29	SPS STOP
96	21	20	21	29	ERRONEOUS SPS TIMING
97	7	42	10	12	SPS CHECK
97	14	38	15	7	SPS STOP
97	20	35	21	55	SPS STOP
99	11	14	11	29	MPX/LATE
99	19	44	20	26	SPS STOP
99	20	56	21	6	ERRONEOUS SPS TIME
101	5	29	6	21	SPS STOP
101	11	56	12	22	SPS CHECK
101	16	32	16	49	SPS STOP
102	6	48	6	57	SPS/EOC TESTS
102	8	30	14	38	SPS CHECK
102	21	26	22	51	SPS STOP
103	9	51	10	4	SPS STOP
103	18	23	18	37	MAINTENANCE
103	20	45	21	26	SPS STOP
104	10	9	10	15	SPS/EOC TESTS
104	12	23	12	37	SPS STOP
104	13	10	13	22	SPS STOP
104	14	21	14	36	SPS STOP
104	15	37	16	46	SPS STOP
107	8	30	8	35	ERRONEOUS SPS TIME
108	11	16	11	26	SPS STOP
108	21	38	23	56	SPS STOP
109	9	21	9	35	SPS STOP
109	16	0	16	13	MAINTENANCE
110	12	35	12	45	SPS STOP
111	7	32	10	13	SPS MAINTENANCE
111	20	55	22	10	SPS STOP
112	11	26	11	42	ERRONEOUS SPS TIME
114	9	19	9	49	SPS MAINTENANCE
114	22	12	22	21	ERRONEOUS SPS TIME
115	13	43	14	12	POWER BREAK
115	14	20	14	31	SPS DOWN WHEN EOC UP
115	19	50	20	50	SPS STOP
115	21	30	22	33	SPS STOP
115	23	36	24	0	SPS STOP
116	0	0	24	0	SPS STOP

TABLE II.1.1

Sheet 1 of 4

LIST OF BREAKS IN DP PROCESSING THE LAST HALF-YEAR

DAY	START		STOP		COMMENTS...........
117	0	0	22	2	SPS STOP
118	8	2	13	58	SPS MAINTENANCE
118	23	30	24	0	MPX/LATE
119	0	0	0	8	MPX/LATE
120	11	13	12	23	MPX/LATE
124	0	15	1	41	SPS STOP
125	6	47	7	12	POSSIBLE PROGRAM ERROR
133	6	41	8	55	POSSIBLE PROGRAM ERROR
136	12	5	12	9	SPS WHEN EOC INTERRUPT
137	5	51	7	39	SPS STOP
138	6	31	7	7	SPS STOP
138	11	43	24	0	POWER BREAK,SPS ERROR
139	0	0	24	0	SPS ERROR
140	0	0	24	0	SPS ERROR
141	0	0	24	0	SPS ERROR
142	0	0	12	22	SPS ERROR
142	13	40	13	54	SPS ERROR
142	14	37	15	31	SPS ERROR
142	19	17	19	53	POWER BREAK
143	0	13	0	46	SPS
143	8	19	9	3	SPS
143	9	18	9	25	MAINTENANCE
145	7	53	8	0	MPX/LATE
146	23	25	23	33	POSSIBLE PROGRAM ERROR
148	2	11	2	56	SPS STOP
149	14	1	14	28	SPS STOP
151	15	1	17	52	POWER BREAK
152	6	59	7	26	SPS STOP
152	8	15	9	16	SPS STOP
157	7	3	7	13	SPS STOP
163	12	6	12	31	MPX/LATE
163	12	53	13	3	MPX/LATE
164	7	46	7	51	POSSIBLE PROGRAM ERROR
164	10	50	10	58	MPX/LATE
164	13	7	14	5	MAINTENANCE
166	16	32	18	20	SPS STOP
169	2	34	3	40	SPS STOP
179	22	4	22	27	POSSIBLE PROGRAM ERROR
181	22	6	22	33	MPX/LATE
184	9	27	9	35	MPX/LATE
186	17	55	21	55	1052 ERROR,A TO B
187	12	54	13	5	B TO A
188	9	59	10	24	POSSIBLE PROGRAM ERROR
188	11	48	12	6	POSSIBLE PROGRAM ERROR
188	13	48	13	54	TOD ERROR
190	6	34	7	42	SPS STOP
191	11	24	11	34	MAINTENANCE,A TO B
191	11	56	13	21	MAINTENANCE
191	15	40	16	10	HARDWARE ERROR

TABLE II.1.1

Sheet 2 of 4

LIST OF BREAKS IN DP PROCESSING THE LAST HALF-YEAR

DAY	START		STOP		COMMENTS...........
192	12	55	13	46	MAINTENANCE
193	10	53	11	36	B TO A
199	20	2	20	13	POSSIBLE PROGRAM ERROR
199	22	12	22	34	MPX/LATE
201	14	5	17	29	POWER BRAK
202	10	23	10	41	MPX/LATE
206	14	13	14	34	POSSIBLE PROGRAM ERROR
208	10	58	14	35	POWER BREAK/PROG. MAINT
209	8	52	8	58	ARPANET HANGUP
✓ 213	20	34	21	48	POWER BREAK
214	6	14	6	44	SPS/EOC TESTS
215	10	35	11	31	DISK CONTROLLER
216	6	41	7	1	SPS/EOC TESTS
219	7	13	7	55	POWER BREAK
221	12	22	12	27	SPS/EOC TESTS
223	17	53	18	12	SPS/EOC TESTS
226	6	47	8	48	POWER BREAK
226	10	20	12	51	MAINTENANCE
227	12	6	13	21	POSSIBLE PROGRAM ERROR
227	23	40	24	0	POSSIBLE PROGRAM ERROR
228	0	0	0	47	POSSIBLE PROGRAM ERROR
228	3	54	7	41	POSSIBLE PROGRAM ERROR
229	8	15	9	33	MAINTENANCE
233	6	26	6	56	MPX/LATE
235	7	35	7	41	MPX/LATE
236	13	46	14	4	DISK HARDWARE ERROR
244	7	37	7	45	SPS STOP
✓ 247	23	13	24	0	SPS STOP
248	0	0	0	1	SPS STOP
249	10	5	10	39	SPS STOP
249	11	35	12	44	SPS STOP
✓ 249	17	47	20	9	SPS STOP
✓ 249	20	15	20	43	SPS STOP
✓ 250	4	0	4	54	SPS STOP
250	9	7	10	8	TAPE CONTROLLER FAILURE
250	10	13	10	38	SPS STOP
✓ 250	19	6	19	46	SPS STOP
250	19	58	21	11	SPS STOP
✓ 250	23	48	24	0	SPS STOP
✓ 251	0	0	1	10	SPS STOP
251	11	28	12	11	SPS STOP
251	12	55	13	17	SPS STOP
✓ 252	6	32	7	22	SPS STOP
252	11	28	12	40	SPS STOP
✓ 252	21	33	22	17	SPS STOP
✓ 252	23	41	24	0	SPS STOP
253	0	0	0	29	SPS STOP

TABLE II.1.1

Sheet 3 of 4

LIST OF BREAKS IN DP PROCESSING THE LAST HALF-YEAR

DAY	START		STOP		COMMENTS..........
√ 254	17	36	18	28	SPS STOP
260	10	13	11	26	POWER FAILURE
261	13	12	13	37	MPX/LATE
261	13	40	13	52	TAPE DRIVE FAILURE
263	8	13	8	37	MPX/LATE
264	9	1	9	27	MPX/LATE
264	17	51	24	0	TAPE DRIVE/CONTROLLER F
265	0	0	7	48	TAPE DRIVE/CONTROLLER F
268	13	46	14	0	EOC,POWER DOWN
269	4	44	6	22	TOD STOP
√ 270	1	33	2	15	SPS STOP
273	7	37	8	49	TAPE DRIVE FAILURE

TABLE II.1.1

Sheet 4 of 4

MONTH	DP UPTIME (Hrs)	DP UPTIME (%)	NO. OF DP BREAKS	NO. OF DAYS WITH BREAKS	DP MTBF* (Days)
APR	635.1	88.2	45	21	0.6
MAY	633.4	85.1	18	16	1.4
JUN	712.9	99.0	12	8	2.3
JUL	725.8	97.5	19	14	1.5
AUG	727.0	97.7	16	14	1.8
SEP	683.0	94.9	29	18	0.9
THE TOTAL PERIOD	4117.2	93.7	139	91	1.2

* Mean-time-between-failures = (Total uptime/No. of Up Intervals).

TABLE II.1.2

Online System Performance

April-September 1978

INTERVAL	INTERVAL UPTIME (HRS)	COHERENT			INCOHERENT			AVERAGE DETECTION RATE (DET./DAY)		AVERAGE OEP EVENT RATE (EVENT/DAY)	
		AVG LTA	NO. OF DETECTIONS	NO. OF OEP EVENTS	AVG. LTA	NO. OF DETECTIONS	NO. OF OEP EVENTS	COH.	INCOH.	COH.	INCOH.
92/11.26-96/15.40	99	631	426	75	737	220	13	103	53	18	3
181/08.13-187/12.21	142	547	547	141	464	651	21	93	110	24	4
243/08.04-249/09.59	145	702	905	124	622	489	20	150	81	21	3

TABLE II.1.3

Detection and Event Statistics for the Online (DP) System,

Selected Intervals

II.2 Event Processor Operation

The operation of the Event Processor was, after a one-year break, resumed as of 1 October 1977. Some statistics for the present reporting period are given in Table II.2.1, where it can be seen that an average of 10.8 events are reported in the NORSAR bulletin per day during the period.

Based on the one year of data now available after the automatic NORSAR event processor was implemented, an analysis of the detection and location capability of the array has been undertaken. Preliminary results from this analysis are given in Section VI.1 and VI.2.

H. Bungum
P. Engebretsen

	Teleseismic	Core Phases	Sum	Daily
Apr 78	275	41	316	10.5
May 78	286	51	337	10.9
Jun 78	336	51	387	12.9
Jul 78	305	56	361	11.6
Aug 78	241	60	301	9.7
Sep 78	201	75	276	9.2
Apr-Sep 78	1644	334	1978	10.8

Table II.2.1

II.3 NORSAR Data Processing Center (NDPC) Operation

Data Center

It has now become clear that one shift of computer operation is not sufficient to handle the combined load of operations and research activities at NORSAR. It is often necessary to run jobs that take an hour or more in the evening. A previous employee has therefore been hired on an hourly basis to run the Data Retention program at night and on the weekends, as this work has fallen far behind schedule. Also during the summer extra help was hired to fill in during vacations.

The DP uptime for the period is 93.7%, which is 2.1% better than last period. There have been two major breakdowns on the SPS, and those breakdowns account for more than half the downtime. The number of stops has not gone down though.

After the reduction in IBM's maintenance contract, the servicing of 10 out of the 15 tape units is now being taken care of by NORSAR personnel. NORSAR personnel have also been engaged in maintenance and problem solving for the SPS, EOC and 360B computer.

J. Torstveit

Array Communications Circuits

Outages when groups of circuits have been affected simultaneously have been few this period. Twenty-one outages of this kind were observed, of which three lasted more than 1 hour. They are as follows:

April	1 outage	Lasted 1 hour
May	6 outages	Of which 1 lasted approx. 2 hours 25.5)
June	4 outages	Of which 1 lasted approx. 1.5 hours 7.6)
July	2 outages	Short
August	5 outages	Short
September	3 outages	Short.

On the other hand, we have experienced single subarray outages of rather long duration, and quite a few have been affected. Reasons have been: cable damages, equalizer trouble, level outside tolerances and reasons not stated. Subarrays particularly affected are:

01A	Week 14	8.0%
"	Week 15	12.5%
"	Week 25	0.8%
01B	Week 15	13.1%
"	Week 25	0.8%
02B	Week 38	15.5%
02C	Week 28	45.2%
"	Week 30	8.0%
"	Week 31	11.9%
"	Week 34	1.4%
03C	Week 18	8.0%
"	Week 23	35.7%
"	Week 25	2.4%
04C	Week 18	6.5%
"	Week 23	21.4%
"	Week 31	12.8%
06C	Week 25	0.6%
"	Week 27	21.4%
"	Week 28	7.1%
"	Week 33	27.4%

All modems, either located in the CTV's or at the Data Center, have been most reliable. However, in Week 35 a separation filter (AHS-card) had to be replaced in the CTV modem at 01B. Prior to the replacement the output level had been too low.

Table II.3.1 shows outages/degraded performance related to communication circuits.

Sub-array	APR (4) (3-30.4)		MAY (5) (1.5-4.6)		JUN (4) (5.6-2.7)		JUL (4) (3.-30.7)		AUG (5) (1.8-3.9)		SEP (4) (4.-30.9)		AVER.	½ YEAR
	>20	>200	>20	>200	>20	>200	>20	>200	>20	>200	>20	>200	>20	>200
01A	8.4	26.3	0.7	0.5	1.8	2.1	0.8	0.7	0.9	0.7	0.6	-	2.2	5.1
01B	2.3	15.1	0.7	0.5	0.9	1.1	0.4	0.7	0.9	1.2	0.6	-	1.0	3.1
02B	0.7	0.7	1.5	0.7	0.4	2.9	0.6	-	1.4	0.7	0.6	14.9	0.9	3.4
02C	0.6	3.2	2.9	2.6	3.0	8.4	1.6	57.6	1.8	27.3	0.8	-	1.8	16.5
03C	0.2	0.7	4.5	4.4	19.4	57.1	1.2	0.2	0.9	0.5	0.9	0.9	4.5	10.6
04C	0.4	0.7	1.5	4.8	0.6	37.5	1.1	0.5	4.6	1.8	1.1	-	1.6	7.6
06C	0.2	0.7	1.1	0.5	0.2	2.2	0.4	28.7	1.4	29.6	0.8	-	0.7	10.3
AVER.	1.8	6.8	1.8	2.1	3.8	15.9	0.9	12.6	1.7	8.8	0.8	2.3	1.8	8.1
LESS	01A 0.8	01A/01B 1.2			03C 1.2	03C/04C 3.3		02C/06C 0.4		02C/06C 1.0		02B 0.2		

TABLE II.3.1

II.4 The ARPA Subnetwork (i.e., TIP to TIP incl. modems, lines and interfaces)

The London Communications Circuit

This circuit has had a high degree of reliability most of the time. In the beginning of August, however, the 'Marginal Circuit' indicator was frequently initiated, but as 'Good Data' was on simultaneously, the error rate was within specifications. On 3 August, the carrier was lost and remained so until 7 August when the 'Go Slow' action among the British BPO employees was terminated.

The SDAC Communications Circuit

In August and September this circuit was subjected to repeated measurements and tests. According to the Network Control Center (NCC) short breaks in the data stream have been observed frequently. Several attempts have been made to isolate the fault, first of all by means of the looping facilities in the modems on both sides (i.e., DC Bus Back, Audio Bus Back and Modem Check). Also agencies such as ITT (in the USA), NTA (Norwegian Telegraph Administration) and the Codex modem representative (in Oslo) have been engaged. In addition, a representative from BBN (Bolt Beranek and Newman) has been involved. Measurements carried out on the line between NORSAR and SDAC 17 September proved attentuation distortion caused by irregularities in the US.

The Terminal Interface Message Processor (TIP)

Preventive maintenance (PM) has been carried out according to the schedule. The teletype (TTY) is also regularly checked and maintained. In the period thunderstorms and power outages have caused a few problems in connection with the system restart. On 13 and 19 July lightning resulted in damaged cards in the Host Interface no. 3 and the Distant Host Driver. On 27 July, after a drop in the main supply, the machine was impossible to restart, and was down approx. 11 hours. A cross-patch setup in London when the NORSAR TIP was down delayed the system restart. Also on 28 July the TIP caused problems. Several tests/restarts under NCC direction failed. On 14 August the TIP failed again one hour after restart due to main supply outage. When NCC tried to reload, it stopped in the same location each time. On 15 August a BBN representative arrived. The system resumed operation after some outages. On 17 September a BBN representative arrived in connection with problems in the subnetwork. At the same time he modified the IMP ID card, word 4 (this card defines the layout of an IMP, and word 4 now defines modem line speed, instead of satellite interfaces).

TIP Connections

No changes have been made to the IMP portion of the TIP, or the TIP port (LIU) connections since the last reporting period.

O.A. Hansen

III. IMPROVEMENTS AND MODIFICATIONS

III.1 Detection Processor

There have been few, but important, modifications to this system within the reporting period, as described below:

- As indicated in Table II.1.1, there were several stops caused by discovery of wrong timing (i.e., discrepancy between SPS internal time and TOD time) early in this reporting period. This was caused by SPS malfunctioning. However, on such occasions, the only thing done by the system was to write out an error message. Additional logic has now been inserted into the DP system, to make it go down gracefully whenever such a discrepancy between the SPS internal time and the TOD time is detected. In this way registration of data corrupted with erroneous time is prevented. This modification was implemented 28 April.

- The parameters in the system holding the value of the subarray beam number (TALESA) and the single sensor channel number (TALESS) to be transmitted to SDAC for an Online Event was changed 18 May. The new channels transmitted with an Online Event are the subarray beam from 03C (5) and the single sensor 02B00 (18). This change was effected by a CORE card in the initialization deck. Future changes should thus be easy to perform.

- The Online Event number (EPX) system was changed 26 May. The philosophy is that Online stops should not cause gaps or jumps in the sequence of EPX numbers. After modification, the system now updates the EPX counter and uses the updated value every time an event is declared. The updated value is also queued, to be written to the disk. During initialization, the value on disk is read and inserted into the EPX counter as a starting value, thus maintaining continuity in the EPX numbers. The only situation that will cause problems is when the system goes down between updating the EPX counter and the actual writing of the updated value to disk. This will lead to duplicate EPXes (before and after the break). However, the first of the events with identical EPX will then probably be incompletely transmitted and registered on tape.

- On 27 July a programming error was found and corrected in the ARPANET message generating module (PNRSAD). Although this error did not influence the effective transmission of ARPANET data, since it occurred only when the local IMP node went 'dead', it prevented the system from staying up on such occasions, when an event was declared.

III.2 Event Processor

The new AUTOEP processing system, which reads Online Event Processor (OEP) results off the Detection Log tape, and performs further processing on these data, has been further improved and modified during the reporting period. Some of the changes have been done in order to adapt and interface it to the Interactive NORSAR Bulletin Editing System (INBES). The AUTOEP-INBES systems now handle all automatic and manual refinement/modification of the OEP solutions (see Fig. III.2.1).

The AUTOEP system reads the OEP results from the Detection Log tape, does solution refinement and computes event parameters. It produces Detection/Event Lists, Event Plots and a first version of an Event Bulletin. A reformatted version of this bulletin, adapted for telex transmission, is also produced. The Event Bulletin is finally written to the Disk Bulletin File. The INBES system allows the analyst to interactively review and modify entries in the bulletin, using the 2260 Display Station as his tool. If an event parameter is modified by the analyst, then automatic re-computation of related parameters will be performed. The final result is an Edited Bulletin, which has been reviewed by the analyst. This bulletin may be extracted (printed & punched) at regular intervals (say, each week).

The following changes have been made to the AUTOEP system:

- A subroutine was added (EDIT) to re-format the bulletin lines, so they conform to the Disk Bulletin File format. (8 May).
- Event statistics showed that the AUTOEP automatic onset selection on the average was 0.6 seconds too late. As an ad-hoc solution, the code was therefore changed to subtract 6 from the sample number returned from the onset selection subroutine. (12 September).

- Code was inserted to check for bad input data (i.e., flat trace), so that division by zero and plotter problems were prevented. (21 September).
- Clipping of traces with amplitudes too large for the allocated interval on the plot was implemented, as an extra security measure against cases of 'gallopping plotter pen'. (21 September).
- The area allocated for each trace was enlarged, so as to increase the amplitude resolution. This was wanted by the analysts. (21 September).

D. Rieber-Mohn

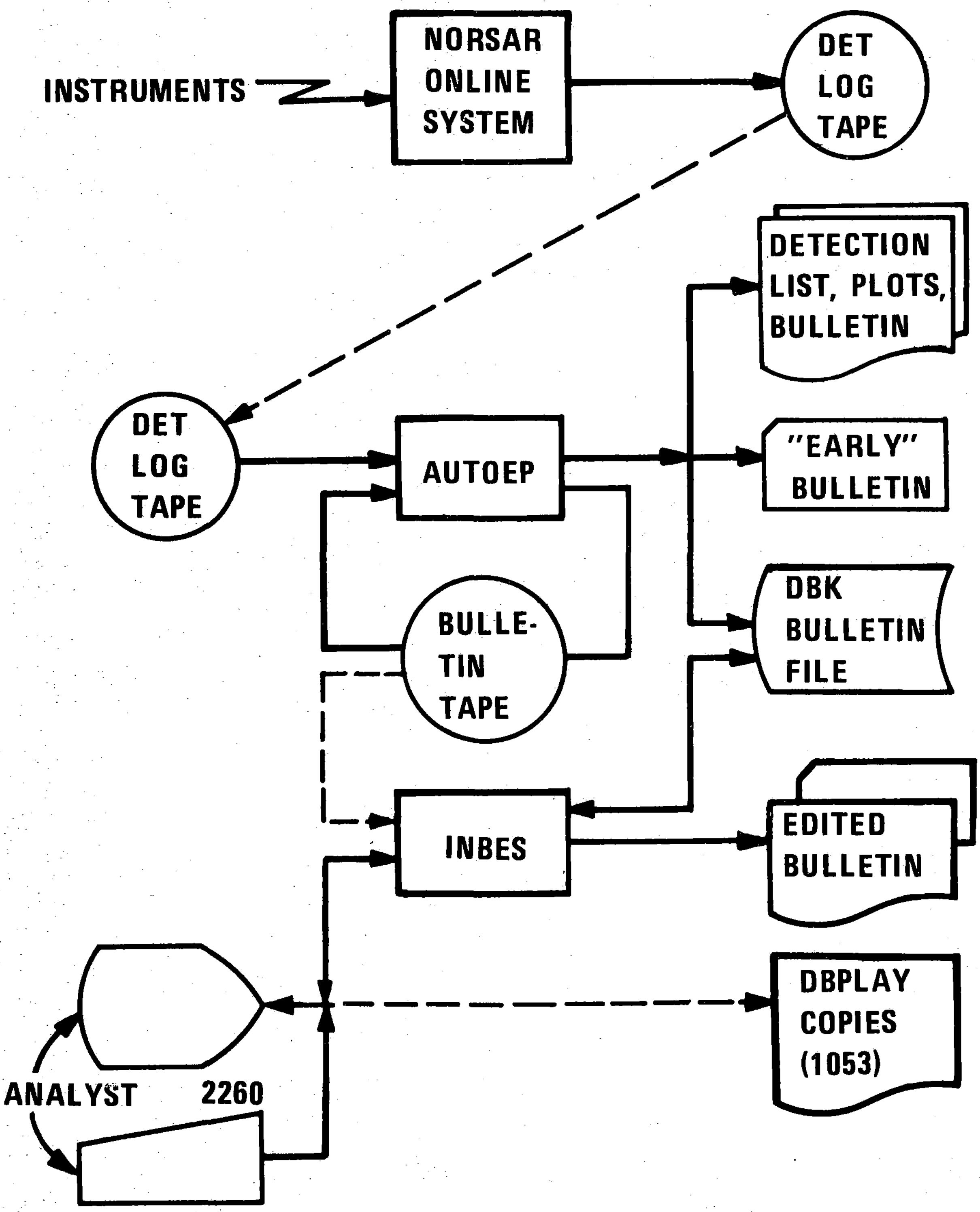

Fig. III.2.1 Data flow in the AUTOEP-INBES system

III.3 Array Instrumentation and Facilities

The test out of a Teledyne Geotech S-500 seismometer initiated 15 March 1978 on 06C channel 02 and described in the last Semi-annual Technical Summary continued from 30 March to 12 April placed in NS horizontal position. A technical report (Larsen, 1978) has been written describing the experiment, whereof the frequency response measurement is copied in Fig. III.3.1.

As of 5 April 1978 a three-axis seismometer system was installed on channels 01 (vertical), 02 (NS horizontal) and 03 (EW horizontal) at subarray 01A in the long period vault, position latitude $60^{o}50'39.2''$ longitude $10^{o}53'11.5''$, elevation 426 meters. The seismometers are Teledyne Geotech S-13 short period seismometers, connected to NORSAR standard channel equipment. Frequency response curve for the vertical channel is given in Fig. III.3.2 and in Table III.3.1 the corresponding numbers are given, including the numbers for NS and EW channels. The calculation of equivalent earth motion and channel resolution is as follows:

Input calibration voltage E_i = 20 VPP

Calibration network resistance R_n = 50 KΩ

Calibration coil resistance R_c = $\underline{23\ \Omega}$

Calibration coil current $I_c = \frac{E_i}{R_n+R_c} \approx \underline{400\ \mu A}$

Calibration coil motor constant G_c = 0.1975 N/A

(for vertical seismometer 0.1973).

Equivalent earth motion at 1.0 Hz in microns:

$$y = \frac{G_c \cdot i \cdot 10^6}{4\pi^2 \cdot f^2 \cdot m}$$

where

y	=	equivalent earth motion in microns, peak-to-peak
G	=	calibration coil motor constant, newtons/ampere
i	=	current through the calibration coil, amperes peak-to-peak
f	=	frequency of calibration signal
m	=	weight of mass i kilograms.

$$y = \frac{0.1975 \cdot 400 \cdot 10^{-6} \cdot 10^{6}}{4 \cdot 9.8696 \cdot 1 \cdot 5} \approx \underline{.400\ \mu\text{M P-P}}$$

Channel resolution at 1.0 Hz:

$$\frac{\text{Equivalent earth motion}}{\text{Quantum units (QU) P-P at channel output}} = \frac{.400}{9360} = \underline{42.73\ \text{PM/QU.}}$$

A.K. Nilsen

Reference

Larsen, P.W. (1978): Test of Teledyne-Geotech S-500 Seismometer, NORSAR Internal Report 1-78/79, in press.

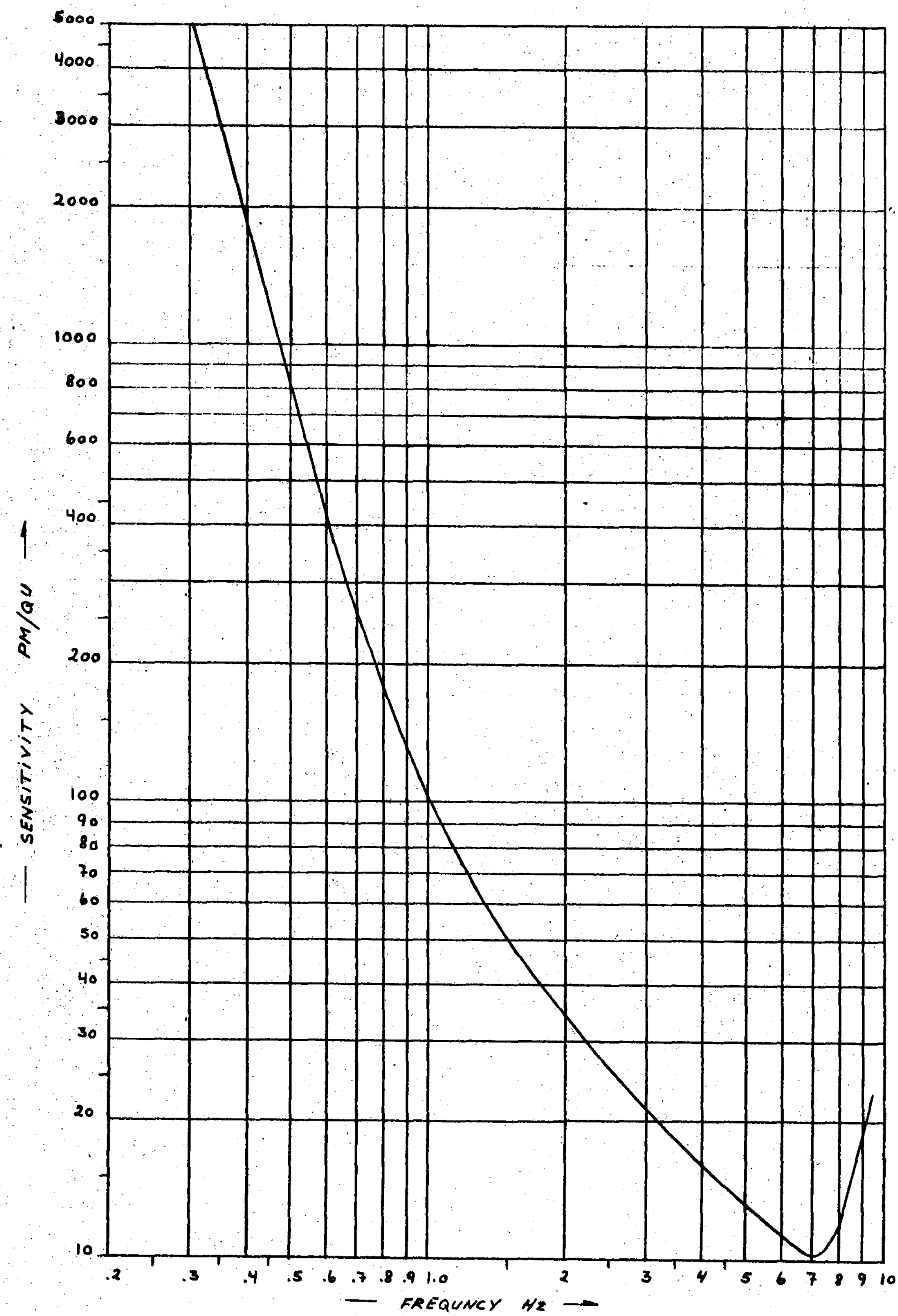

Fig. III.3.1 S-500 frequency response.

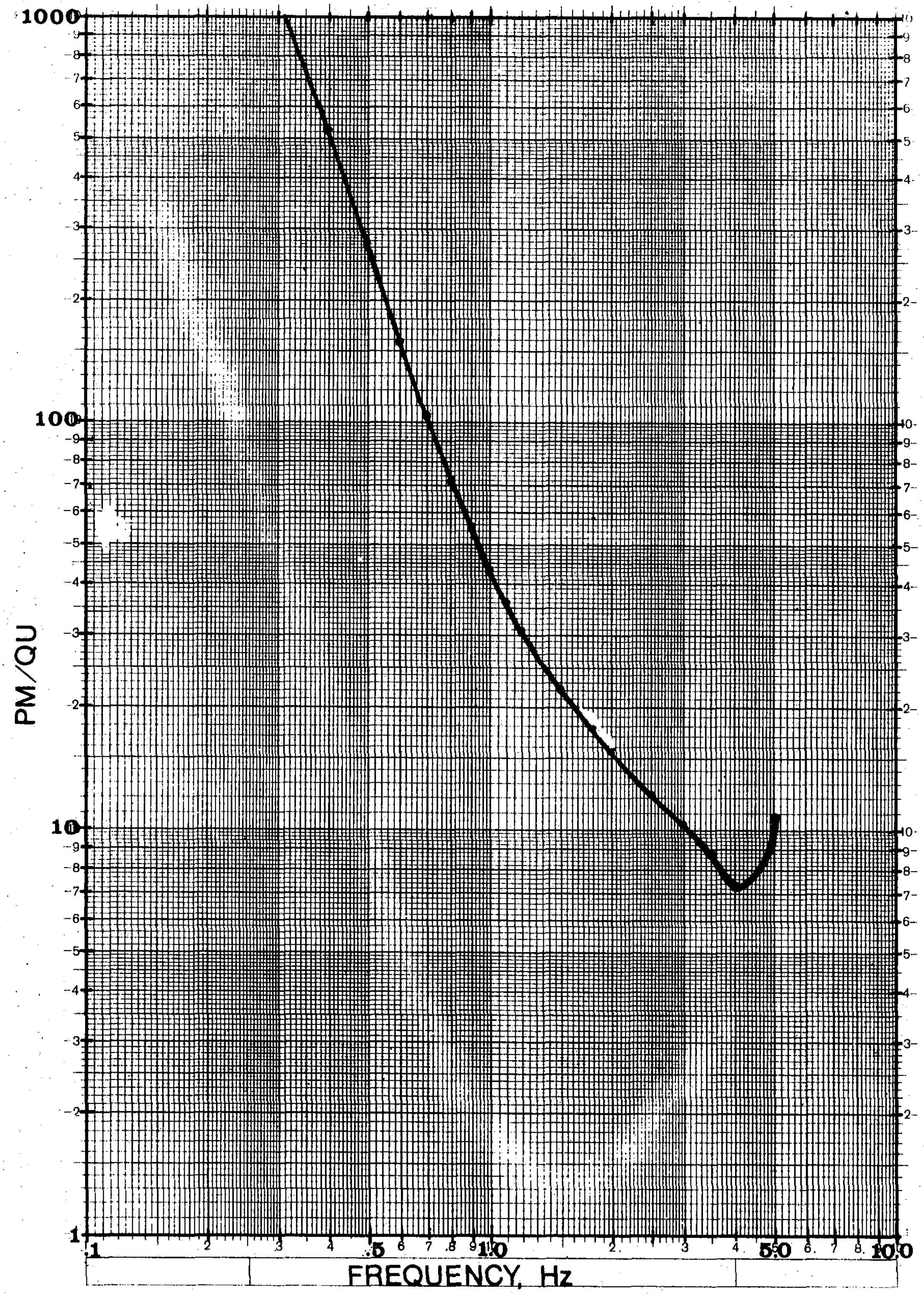

Fig. III.3.2 S-13 V frequency response.

Frequency Hz	Output of ADC, PM/QU		
	01A01 (V)	01A 02 (NS)	01A 03 (EW)
0.1	48777	48826	40689
0.2	5081	4694	4069
0.3	1355	1292	1356
0.4	525.6	544.9	544.9
0.5	278.0	271.3	271.3
0.6	157.55	157.71	157.71
0.7	103.69	99.65	101.68
0.8	71.90	69.36	71.97
0.9	54.74	53.82	53.82
1.0	42.73	42.73	42.73
1.1	35.99	36.03	35.40
1.2	30.79	30.82	30.82
1.5	22.12	21.70	22.14
2.0	15.63	15.65	15.65
2.5	12.19	12.21	12.21
3.0	10.42	10.43	10.05
3.5	8.66	8.66	8.66
4.0	7.26	7.27	7.63
4.75	8.32	8.32	9.02
5.0	10.84	10.85	10.85

TABLE III.3.1

Frequency response of three-axis seismometer
at 01A as of 26 July 1978

IV. MAINTENANCE ACTIVITY

A brief review of the maintenance activity at the subarrays by the field technicians as a result of the remote array monitoring and routine inspection is given. The main preventive work in the period is dryout and painting of the floor and long period tanks in some of the long period vaults and replacement of seismometer amplifiers due to decaying battery power.

Maintenance Visits

Fig. IV.1 shows the number of visits to the subarrays in the period, in average each subarray has been visited 9.3 times. The large number of visits to 06C are due to cable breakages. The relatively high number of visits is mainly explained by the preventive work mentioned above.

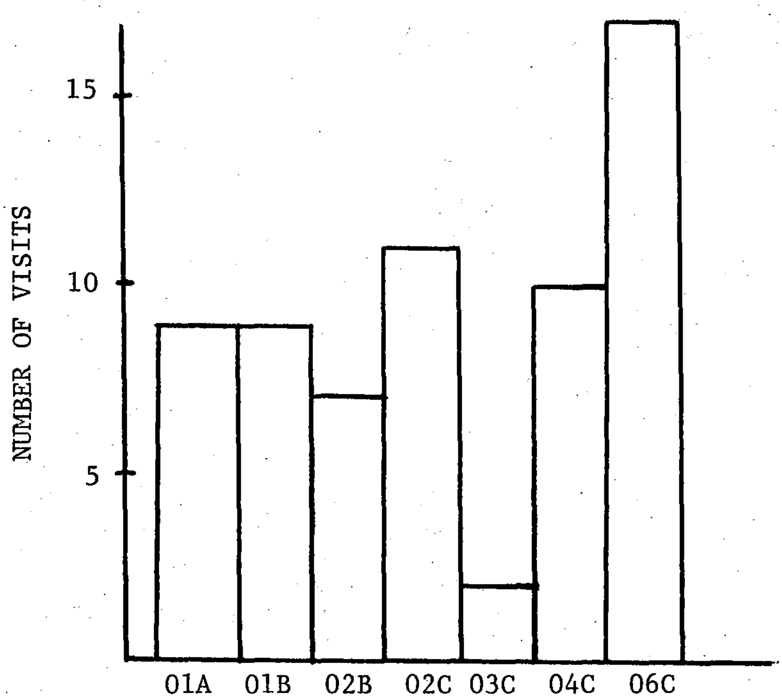

Fig. IV.1 Number of visits to the NORSAR subarrays in the period 1 April to 30 September 1978.

Preventive Maintenance Projects

The preventive maintenance work in the array is described in Table IV.1. The adjustments are corrections of characteristics within the tolerance limits.

Unit	Action		No. of Actions
LTA	Adjustment of DC offset	SP	15
		LP	2
	Adjustment of channel gain	SP	5
		LP	4
	Adjustment of CMR	LP	3
Seism. Amplifier	RA-5 replaced due to decaying battery power		15
Seis-mometer	MP adjustment (in field)		9
	FP adjustment (in field)		7
SLEM	RSA/ADC adjustment		1
Facilities	Dryout and painting of LPV and LP tanks including replacement of RCD's.		3
CTV/LPV Access Roads	Sprayed with chemicals against bushes		6

TABLE IV.1

Preventive Maintenance Work in the Period

1 April to 30 September 1978

Disclosed Malfunctions on Instrumentation and Electronics

Table IV.2 gives the number of accomplished adjustments and replacements of field equipment in the array with the exception of those mentioned in Table IV.1.

Unit	Characteristic	SP Repl.	SP Adj.	LP Repl.	LP Adj.
Seis-mometer	Damping		3		
	MP (field)				10
	FP (field)				7
Seism. Ampl. RA-5/ Ithaco	Balance			1	
	Gain	1			
LTA	DCO		4		1
	Ch. Gain		4		2
	CMR		1		

TABLE IV.2

Total number of required adjustments and replacements in the NORSAR data channels and SLEM electronics

(1 April - 30 September 1978)

Malfunction of Rectifiers, Power Loss, Cable Breakages

There has been no malfunction of the rectifiers in the period, or power loss requiring action of the field technicians. The number of cable breakages was 15, requiring 15 days' work.

Array Status

The status of the array characteristics is similar to previous periods with little change. The SP array average DC offset was -3.4 millivolts averaging four minutes of quiet background noise. The LP DC offset was -0.5 millivolts over a ten-minute period.

A. Kr. Nilsen

ABBREVIATIONS

ADC	-	Analog to digital converter
CMR	-	Common mode rejection
CTV	-	Central Terminal Vault
DC	-	Direct current
DCO	-	DC offset
FP	-	Free period
LP	-	Long period
LPV	-	Long period vault
LTA	-	Line termination amplifier
MP	-	Mass position
PM	-	Pico meter
QU	-	Quantum units
RCD	-	Remote centering device
RSA	-	Range switching amplifier
SLEM	-	Short and long period electronics modules
SP	-	Short period.

V. DOCUMENTATION DEVELOPED

V.1 Reports, Papers

Bungum, H. (1978): Re-analyzation of three focal-mechanism solutions for earthquakes from Jan Mayen, Iceland and Svalbard, Tectonophysics, in press.

Gjøystdal, H. (1978): Semiannual Technical Summary, 1 October 77 - 30 April 1978, NORSAR Scientific Report 2-77/78.

Haddon, R.A.W. (1978): Scattering of seismic body waves by small random inhomogeneities in the earth, NORSAR Scientific Report No.3-77/78.

Larsen, P.W. (1978): Test of Teledyne-Geotech S-500 seismometer, NORSAR Internal Report No. 1-78/79.

Rieber-Mohn, D. (1978): The Interactive NORSAR Bulletin Editing System - User Guide and Documentation, NORSAR Internal Report No. 3-77/78.

L.B. Tronrud

V.2 Program Documentation

Documentation N/PD-93 has been completed within this period. N/PD-93 is a subroutine that reads tapes produced by the DHR-1632 recording system.

D. Rieber-Mohn

VI. SUMMARY OF SPECIAL TECHNICAL REPORTS/PAPERS PREPARED

VI.1 Evaluation of the Current NORSAR Detection Capabilities

One year of analyzed data (Oct 77-Sep 78) is now available after the NORSAR array was reduced in size. This data base is considered sufficient to conduct a preliminary analysis of the capabilities of the new NORSAR configuration. In the present study, the current event detection capabilities have been estimated both by comparison with the old 22 subarray system and by recurrence analysis of the magnitude-frequency relationship of the reported earthquakes.

Table VI.1.1 and Fig. VI.1.1 show the monthly average number of reported events during the last four years of 22 subarrays operation as compared to the most recent year. All of these numbers are based upon events reported in the analyst-reviewed NORSAR seismic bulletin, and thus represent real seismic events with minimal occurrence of false alarms. Apart from one month, March 1978, during which a large earthquake sequence occurred, the picture is quite stable, and the average monthly number of reported events is now about 60% of what it was before the reduction from 22 to 7 subarrays. The ratio is about 65% if one compensates for the increased system downtime after the reconfiguration. From Table VI.1.1 it is further seen that the estimated degradation does not change significantly if one deletes all months that contain large earthquake sequences.

Assuming that the b-value of the magnitude-frequency recurrence relationship is independent of time, it is easily seen that the change in 50% incremental detectability threshold Δm_b corresponding to the ratio R of detected events (in per cent) can be expressed as (Pirhonen et al, 1976)

$$\Delta m_b = -\frac{1}{b} \cdot \log_{10} \left(\frac{R}{100}\right)$$

Assuming b=0.9, R=65 then gives Δm_b=0.21. This may be compared to the theoretical reduction in beamforming gain ΔG for 7 versus 22 subarrays, which is $10 \cdot \log_{10} 22/7 = 5.0$ dB or 0.25 m_b units. Thus the observed performance relative to the old configuration corresponds closely to what could be expected. It appears that the increased automation in the bulletin generation procedure has not significantly affected the detection performance, as far as the number of reported events is concerned.

We now turn to the problem of obtaining an independent measure of the current NORSAR detectability (i.e., a measure not relative to previous capabilities). Our progress so far has been rather limited, because the most reliable estimation method, namely, that of checking detections against an independent reference station (Ringdal, 1975) has not been possible to use after the only reference system of sufficiently high capability, the SDAC/LASA bulletins, has been discontinued. Therefore, we have resorted to the recurrence technique, analyzing the available one year of data (Oct 77 - Sep 78) in a way identical with what was done by Berteussen et al (1976) in their final evaluation of the NORSAR detectability before the reduction in array size. Only the results from the least squares cumulative method will be presented here, as shown in Table VI.1.2. The method is illustrated in Fig. VI.1.2, which shows the combined teleseismic data (Region 14). The results in Table VI.1.2 must be considered relatively uncertain for most regions, due to the limited data base. Nonetheless, we may take note of the 90% cumulative thresholds for regions such as Central Asia (3.6) and Japan-Kamchatka (4.0). It is also evident that the performance has decreased somewhat relative to that of the NORSAR system during 1972-75 (Berteussen et al, 1976), with a degradation varying in the range 0-0.3 m_b units. The uncertainties inherent in the estimation method should, however, not be forgotten, and in general we consider the number of reported events to be a more reliable indicator of the array performance than the results from the recurrence analysis.

Our future plans include developing new methods for a more reliable direct estimation of the detectability of the NORSAR array, in particular at regional and near-regional distances. As more data are accumulated, it should also be possible to obtain better estimates of event detectability in selected seismic regions.

H. Bungum

F. Ringdal

References

Berteussen, K.-A., H. Bungum and F. Ringdal (1976): Re-evaluation of the NORSAR detection and location capabilities. Scientific Report No. 3-75/76, 20 June 1976.

Pirhonen, S.E., F. Ringdal and K.-A. Berteussen (1976): Event detectability of seismograph stations in Fennoscandia. Phys. Earth Planet. Inter., 12, 329-342.

Ringdal, F. (1975): On the estimation of seismic detection thresholds. Bull. Seism. Soc. Amer., 65, 1631-1642.

	(a) 4 yrs	(b) 1 yr	(c) Ratio (R)	(d) log R	(e) Swarms Removed
	72/76	77/78	(%)		(%)
Oct	483	380	79	-0.10	79
Nov	430	214	50	-0.30	49
Dec	505	235	47	-0.33	54
Jan	658	210	32	-0.49	48
Feb	499	263	53	-0.28	53
Mar	513	855	167	0.22	-
Apr	555	316	57	-0.24	60
May	550	337	61	-0.21	65
Jun	769	387	50	-0.30	76
Jul	659	361	55	-0.26	59
Aug	692	301	43	-0.37	57
Sep	442	276	62	-0.21	62
Average	563	345	61	-0.24	60
Average Compensated for DP Down-Time	576	373	65	-0.22	64

Average DP uptime 1972/76: 97.7%

Average DP uptime 1977/78: 92.7%

TABLE VI.1.1

Monthly averages of the number of NORSAR-reported events (a) for the four years Oct 72 - Sep 76, (b) for the year Oct 77 - Sep 78, (c) the ratio R (%) between the numbers, (d) $\log_{10}$ R, (e) the ratio R modified by deleting months during which significant earthquake swarms occurred.

Region	Area of Coverage	Events 1977/78	90% Cumulative	Down from 1972/75
1	Aleutians-Alaska	214	4.0	0.3
2	Western North America	36	-	-
3	Central America	62	4.4	0.1
4	Mid-Atlantic Ridge	52	3.9	0.1
5	Mediterranean-Middle East	259	3.7	0.1
6	Iran-Western Russia	147	3.7	0
7	Central Asia	276	3.6	0.1
8	Southern-Eastern Asia	187	3.9	0.3
9	Ryukuo-Philippines	325	4.5	0
10	Japan-Kamchatka	1255	4.0	0.2
11	New Guinea-Hebrides	105	4.6	0.1
12	Fiji-Kermadec	605	4.1	0.2
13	South America	31	-	-
14	Distance range 30^o-90^o	2815	3.9	0
15	Distance range 110^o-180^o	802	4.7	0.1

TABLE VI.1.2

Detectability statistics for the reconfigured NORSAR array for 15 geographic regions (see Berteussen et al, 1976). Within each region the table gives the number of reported events, the estimated cumulative 90% detection threshold in terms of NORSAR m_b (from recurrence analysis) and the corresponding degradation relative to the 1972/75 performance (as estimated by Berteussen et al, 1976).

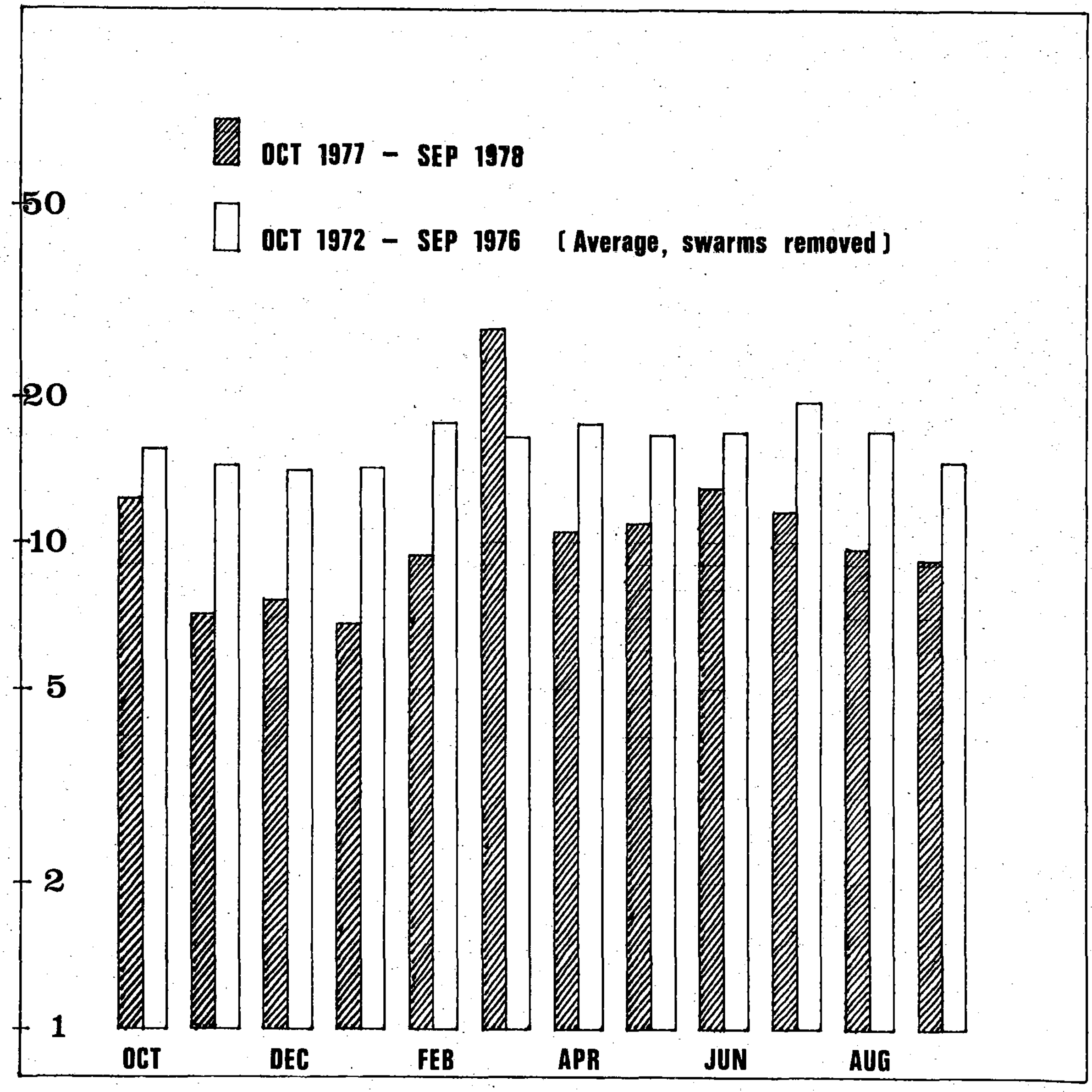

Fig. V.1.1 Monthly averages of reported events at NORSAR, corresponding to the last column of Table VI.1.1. Note that in computing the averages for the period Oct 1972 - Sep 1976 all months with significant earthquake swarms have been ignored. According to the same criterion, the month of March 1978 should be ignored when comparing the two periods.

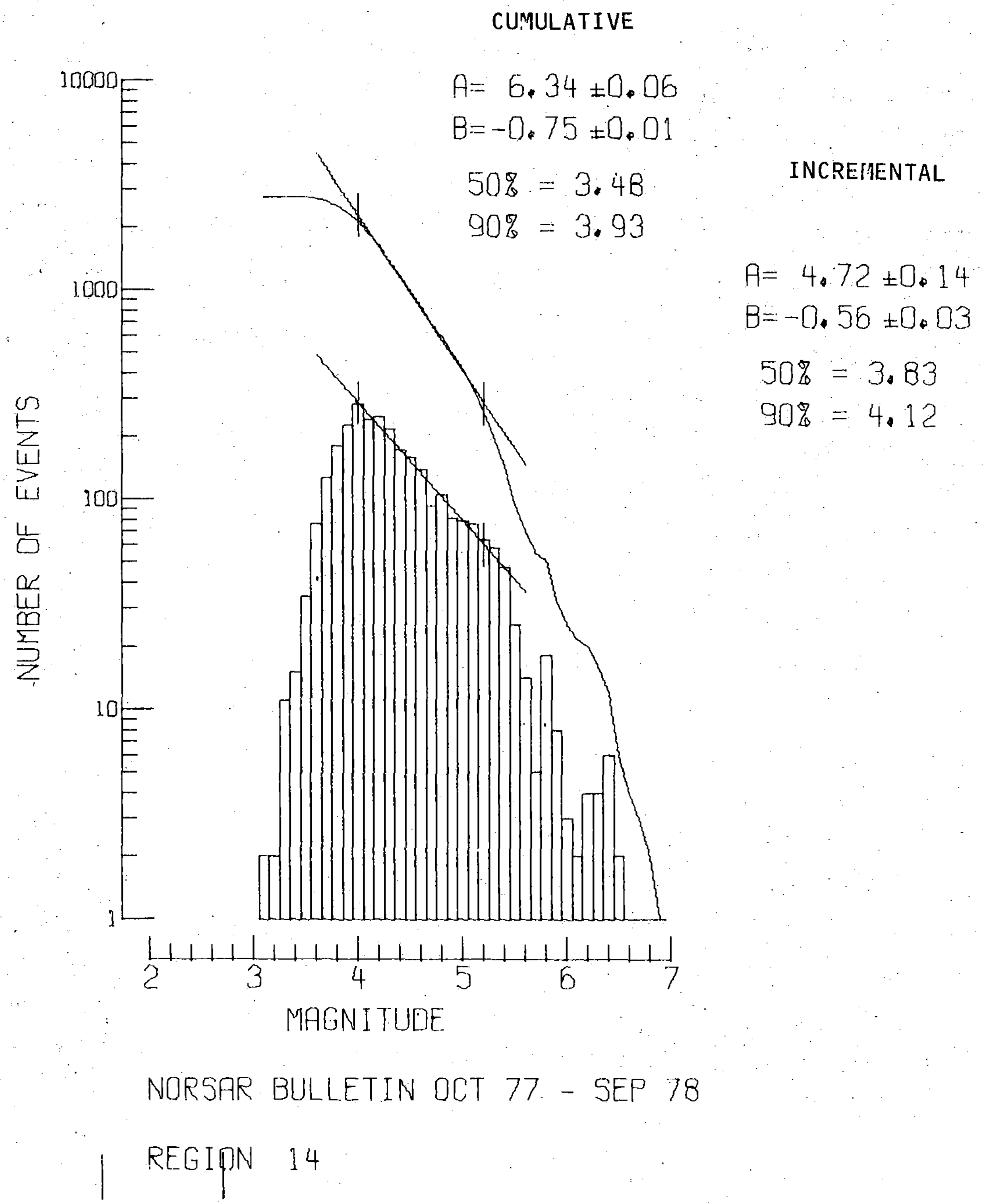

Fig. VI.1.2 Frequency-magnitude distribution for events reported in the NORSAR seismic bulletin for the one-year period October 1977-September 1978. The figure covers events in the distance range 30^{o}-90^{o} from NORSAR. Estimated cumulative and incremental detection thresholds are indicated.

VI.2. Evaluation of the Current NORSAR Location Capabilities

The effect of the reduction in the array size has been investigated by comparing the NORSAR locations with the PDE (Preliminary Determination of Epicenters) from the USGS (United States Geological Survey). Because of the delay in the PDE bulletin, only three months of data have been available for comparison from October 1977 to December 1977.

Fig. VI.2.1 shows the NORSAR/USGS location difference for 286 events commonly reported within teleseismic distance from NORSAR (30^o-90^o). The median location difference is 230 km, which should be compared to the 130 km reported for the same region using the old and larger array (Berteussen et al, 1976). Results on a regionalized basis are shown in Table VI.2.1, where we can see that the increase in the median location difference ranges between 20% and 100% for the different regions. Estimates were not obtained for 6 of the regions because of the limited amounts of data available. We see from the table that while Japan-Kamchatka previously was the best region, it is now Central Asia, with a medium location difference of 170 km.

In considering these results it is important to notice that at the same time as the array was reduced in size (about 50% in diameter), the amount of processing for each event was also reduced, essentially by removing the previous epicentral refinement procedure and using only the beam location from the on-line detection. The effect of the array size reduction itself is therefore smaller than what is reflected in the numbers given in Table VI.2.1.

H. Bungum

Reference

Berteussen, K.-A., H. Bungum and F. Ringdal (1976): Re-evaluation of NORSAR detection and location capabilities, NORSAR Scientified Report 3-75/76.

Regions	Area of Coverage	Jan 73 - Mar 75		Oct 77 - Dec 77		Increase
		Events	Median	Events	Median	(%)
1	Aleutians-Alaska	461	110	38	180	64
2	Western North America	129	130	6	-	-
3	Central America	146	200	6	-	-
4	Mid-Atlantic Ridge	143	150	1	-	-
5	Mediterranean-Middle East	389	300	29	520	73
6	Iran-Western Russia	182	170	11	-	-
7	Central Asia	349	120	32	170	42
8	Southern-Eastern Asia	205	150	21	180	20
9	Ryukuo-Philippines	424	200	39	250	25
10	Japan-Kamchatka	1062	100	82	200	100
11	New Guinea-Hebrides	263	210	10	-	-
12	Fiji-Kermadec	508	230	74	400	74
13	South America	112	210	9	-	-
14	Distance Range 30^{o}-90^{o}	3775	130	286	230	77
15	Distance Range 110^{o}-180^{o}	1195	220	100	380	73

TABLE VI.2.1

Median location difference in km between USGS and NORSAR for the time period Jan 73-Mar 75 (Berteussen et al, 1976) and for Oct 77-Dec 77 (present study), and the increase in percentage.

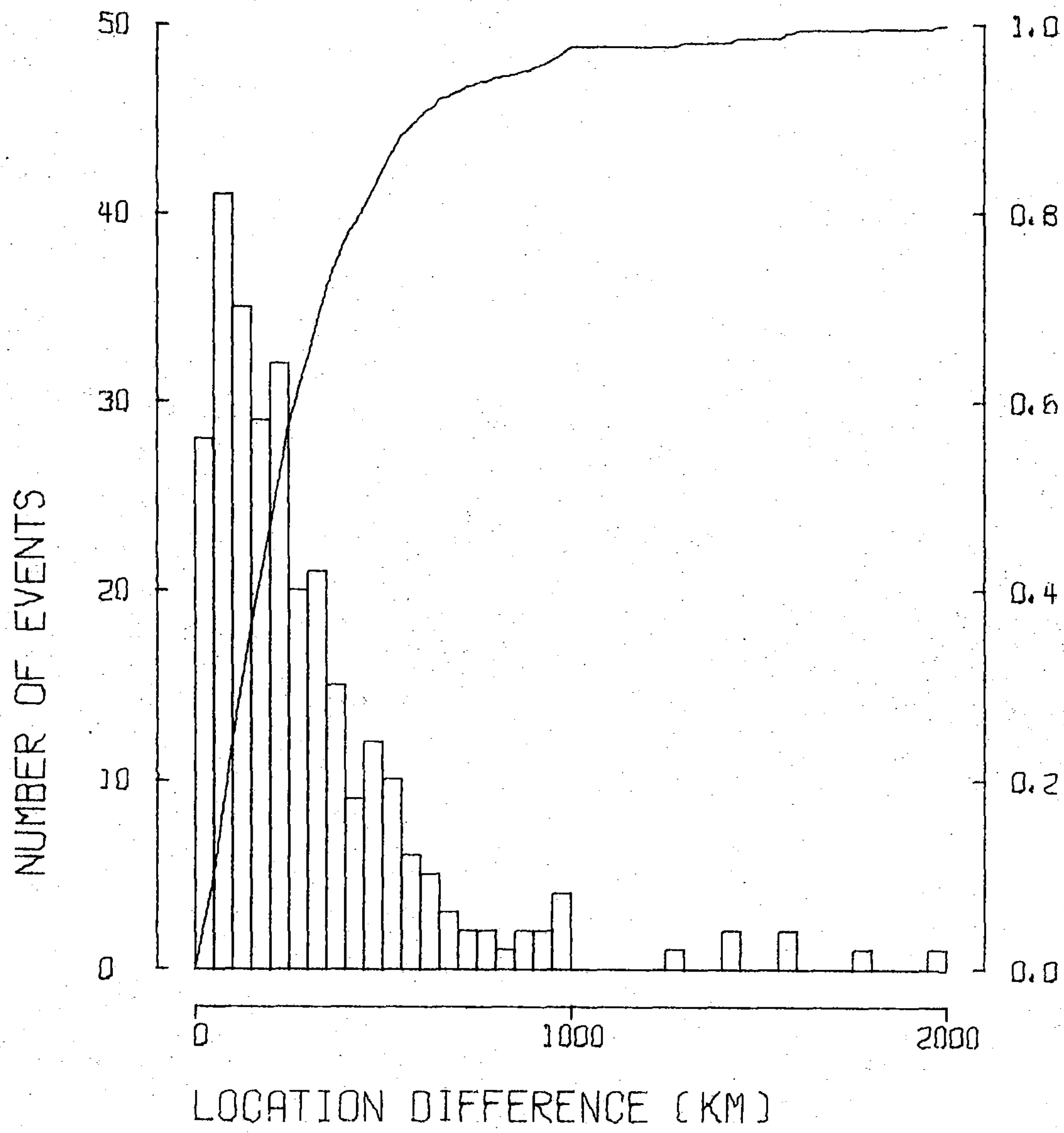

Fig. VI.2.1 Cumulative and incremental distribution of epicenter location differences between USGS and NORSAR for Region 14 (see Table VI.2.1) for the time period Oct 77 - Dec 77.

VI.3 Magnitude Studies

Seismic event magnitude represents one of the most important parameters in the context of seismic discrimination due to the versatility of the $m_b:M_s$ discriminant. A novel approach to the estimation of magnitude was introduced by Ringdal (1976), who pointed out the advantages of using truncated distribution theory in estimating network magnitudes of small events. This topic has been further elaborated by Christoffersson (1978), who developed a unified model for estimating magnitudes and detection thresholds. This approach has now been extended to estimate simultaneously M_s-m_b relation of earthquakes, the scattering in these observations together with detection thresholds for the arrays and individual seismograph stations used to form the data base. In the present study, we have adapted the maximum likelihood technique to assess the linearity or lack of such of the $m_b:M_s$ relationship - a problem critical for seismic source identification. Only preliminary results based on rather limited observational data have been obtained so far, and examples of the observed (m_b,M_s) relations are shown in Figs. VI.3.1 and VI.3.2. These results are based on M_s-values as reported by Uppsala, although we have also experimented with corresponding NOAA and NORSAR observations. In the latter cases, the results are similar to those displayed in Fig. VI.3.1 and VI.3.2. It should be noted here that Uppsala appears to be the only seismological station which consistently reports the M_s-parameter and also has done so over a very extensive period of time. Of course, other seismological agencies like ISC (International Seismological Centre), NOAA (National Oceanic and Atmospheric Administration, USA), Moscow World Data Center and also the Berkeley (BKS) seismographic station often report M_s-magnitudes, but their observations constitute the average for a set of stations, while for BKS the reported M_s is the average of the truly observed M_s and the linearly transformed m_b-to-M_s values.

An illustration of Christoffersson's method applied to m_b data from two stations is shown in Fig. VI.3.3, and it is seen that the apparent deviation from the expected slope of 1.00 can be satisfactorily explained by detectability considerations.

Our studies so far have verified the commonly observed appearance of M_s:m_b scatter plots: at high magnitudes, the M_s:m_b slope is significantly greater than 1.00 (typically around 2), while at lower magnitudes (below $m_b \sim 6.0$) there is apparently a distinct curvature in the relationship between M_s and m_b. However, our results show that this behavior may be explained as a result of bias effects in the plots at low magnitude caused by detectability problems. Thus the hypothesis of an intrinsically linear m_b-M_s relationship with a slope greater than 1.00 even at low magnitudes cannot be rejected on the basis of these and other similar observations. The work reported above will be continued, and future plans include greatly extending the data base so as to allow more specific conclusions about the slope of the M_s-m_b relationship.

A. Christoffersson, Dept. of Statistics, Uppsala
F. Ringdal
C. Bjørck, Dept. of Statistics, Uppsala
E.S. Husebye

References

Christoffersson, A. (1978): Statistical models for seismic magnitude, NORSAR Scientific Report No. 1-77/78, NTNF/NORSAR, Kjeller, Norway.

Ringdal, F. (1976): Maximum-likelihood estimation of seismic magnitude. Bull. Seism. Soc. Amer., 66, 789-802.

Ringdal, F., E.S. Husebye and J. Fyen (1977): Earthquake detectability estimates for 478 globally distributed seismograph stations. Phys. Earth Planet. Inter., 15, P24-P32.

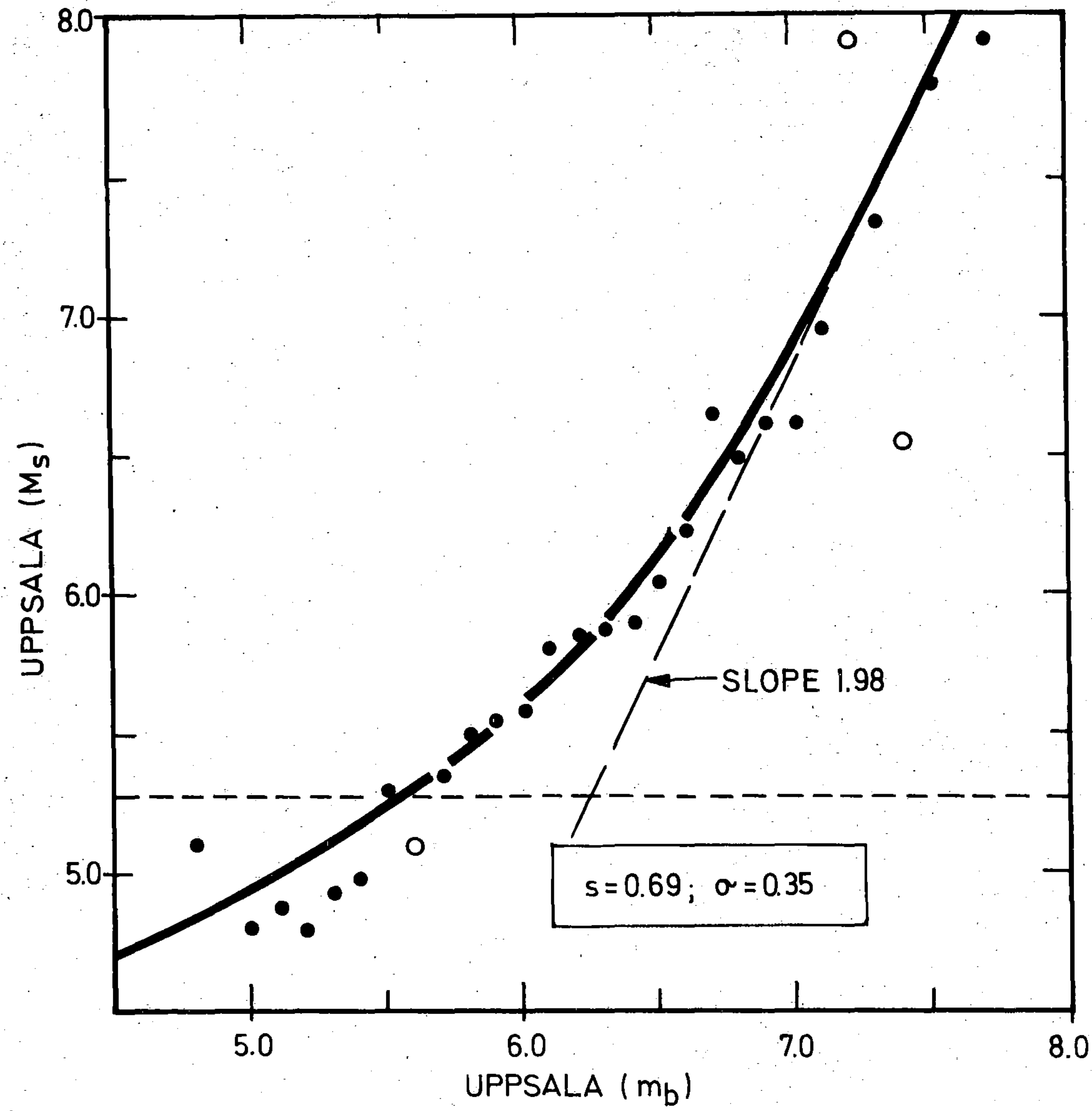

Fig. VI.3.1 Average M_s for given m_b values (both M_s and m_b reported by Uppsala for a reference data set of 412 earthquakes. The solid, curved line is a model fit based upon an assumed linear M_s-m_b relation (slope as indicated) modified by an estimated M_s detectability curve. The parameters (μ,σ) of the detectability curve (Ringdal et al, 1977) are indicated (μ is shown by a stippled horizontal line). The standard deviation S of the inherent M_s-m_b scatter is also estimated. The open circles are data points outside two standard deviations from the model.

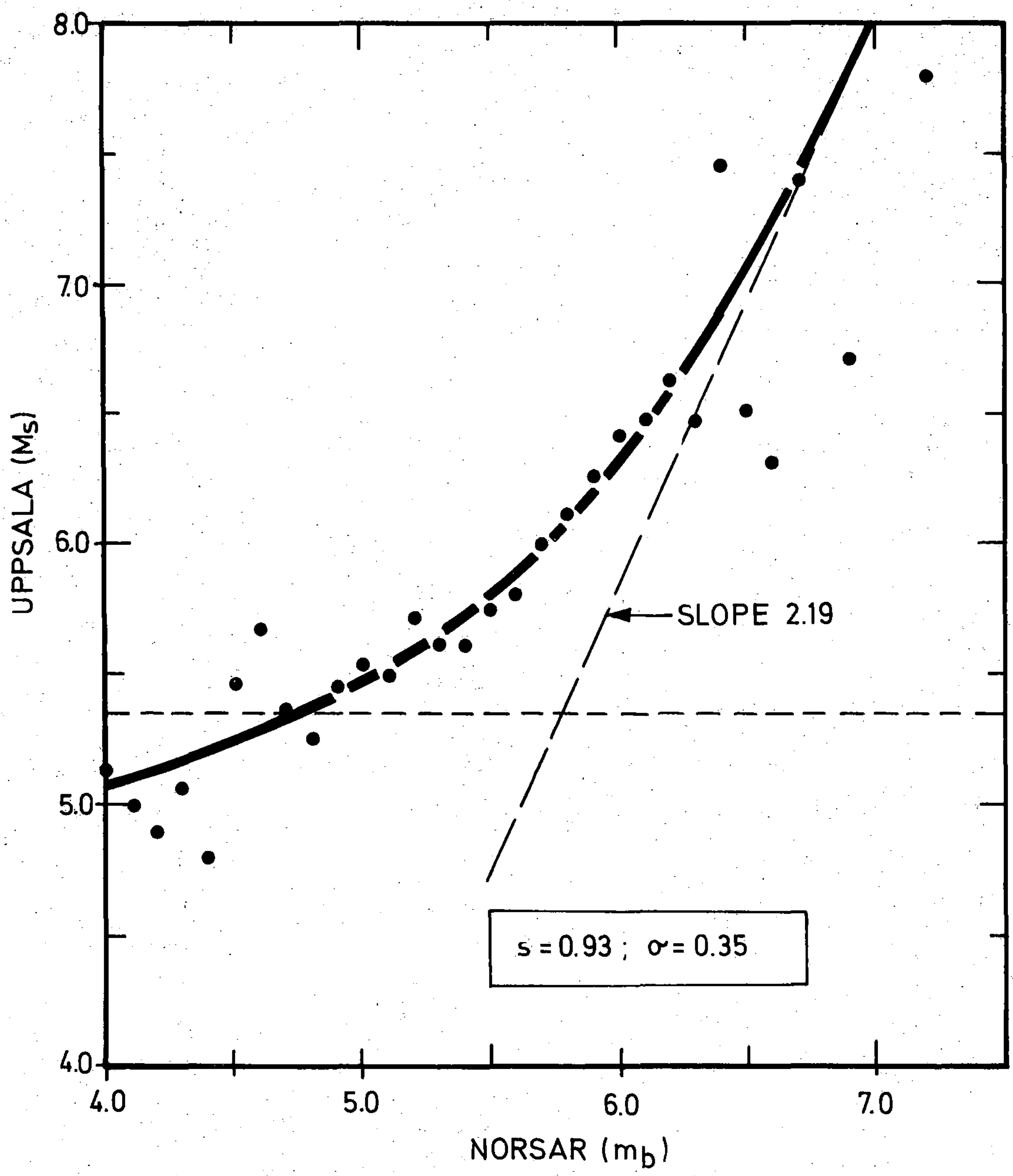

Fig. VI.3.2 Same as Fig. VI.3.1, but with m_b as reported by NORSAR, M_s by Uppsala and the data set containing 403 earthquakes.

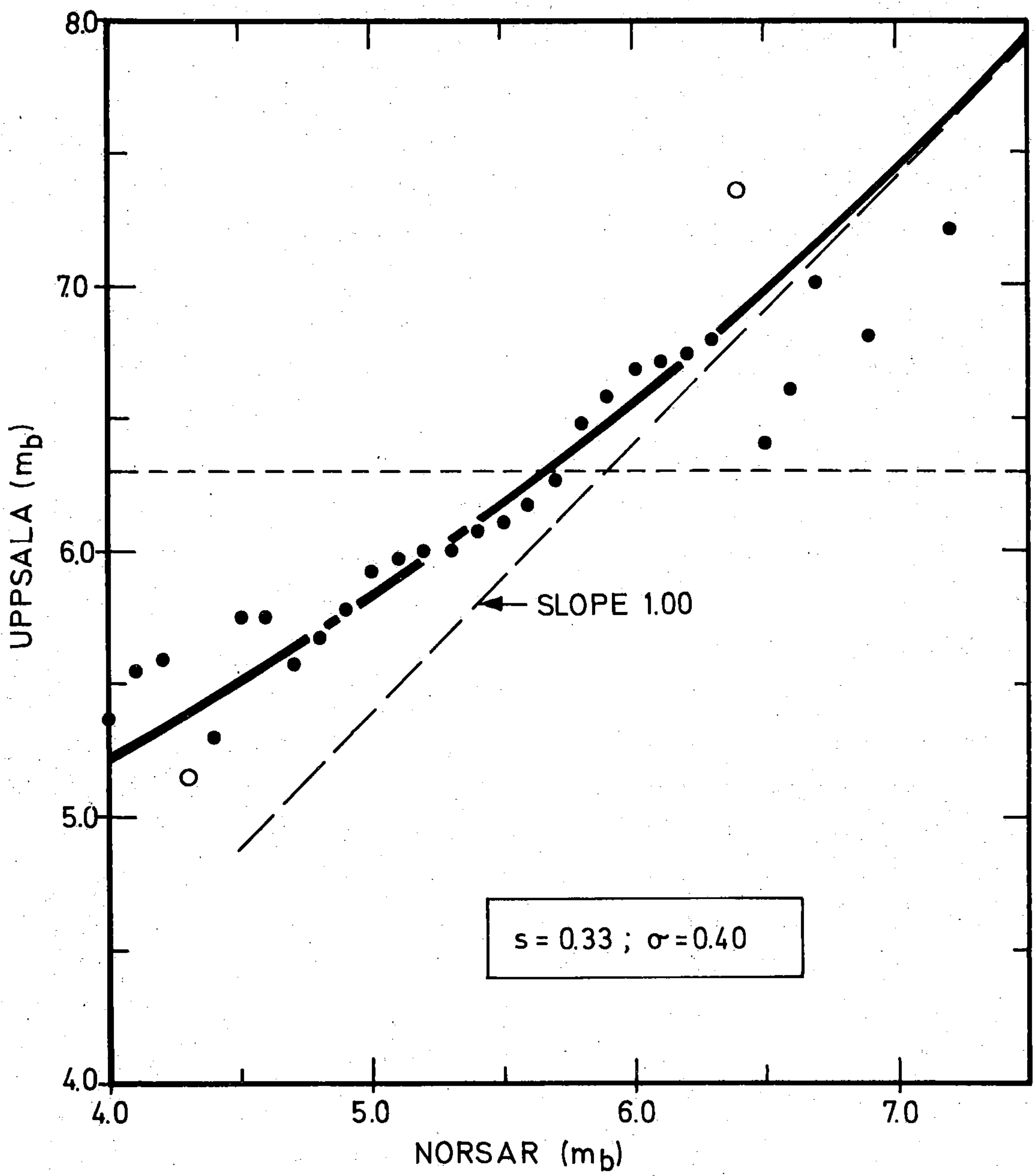

Fig. VI.3.3 Illustration of the model in Fig. VI.3.1 and VI.3.2 applied to estimate the relationship between m_b (NORSAR) and m_b (UPPSALA) (data base 386 earthquakes). The expected slope of 1.00 does <u>not</u> appear to fit the observed data. However, if one takes the effect of detection thresholds into account, while fixing the slope at 1.00, one arrives at the solid, curved line which is a much better fit.

VI.4 Seismic Event Discrimination Based on Near-Field Observations

Up to now the NORSAR event discrimination efforts have to a large extent been based on information extended from teleseismic recordings corresponding to epicentral distances mostly in excess of 30 deg. Lately we have taken up research aimed at several aspects related to seismic event discrimination based on near-field recordings. Although only preliminary results are available at present, we consider it worthwhile to present in some detail the rationale behind these efforts and also the work done so far.

Seismograph Station Detectability Studies in Near-Field Distance Ranges

Most event detectability studies previously undertaken have been based on the reporting performance of individual stations of P-wave recordings in the epicentral distance interval of 30-90 deg. The actual observational data necessary for such studies may be extracted from easily available files, and in this respect the ISC (International Seismological Centre, U.K.) bulletin files have been widely used, e.g., see Ringdal et al (1977). Now, in this approach a prerequisite is that a station reporting performance is somewhat lower than that of the reference station or reference reporting agency like ISC, a condition which with few exceptions is fulfilled for teleseismic distance ranges. For example, out of the 482 stations analyzed using the ISC focal parameters as a reference, only 4 stations had a P-wave reporting performance better than or equivalent to that of ISC, so that their detectability performance could not be estimated reliably. Problems of the latter type may become much more severe for near-field distance ranges, as in this case we have to actually consult individual station bulletins to check on possible mismatches in event detectability with that of ISC. As NORSAR's event detectability performance is superior to that of most other stations and networks for events occurring in large parts of Eurasia, we are considering options to replace ISC by NORSAR as a reference station in the detectability analysis. We are also investigating the possibility of obtaining local station bulletins so as to enable us to undertake specialized analysis of stations of particular interest in this respect.

Work accomplished so far here is as follows:

- All available ISC-bulletin files since 1971 have been transformed to a special compact format suitable for our particular kind of analysis.
- The corresponding data analysis routines have been adapted for detectability estimates for all stations consistently reporting to the ISC and for near-field distance intervals of 5, 10 and 15 deg to ensure that at least in some intervals sufficient data will be available.

We are also considering an extended detectability study based on the fact that stations in coastal and some other areas have an event detectability which is likely to be subjected to seasonal weather conditions. In other words, we are considering estimating station detectability as a function of time of year in intervals of 3 months. The outcome of this experiment will be used for checking whether there is a significant difference in event detectability of certain areas at high latitudes by using an appropriate network of high-quality seismograph stations.

Present status on the various detectability experiments is that the necessary software developments have been completed, and that the first analysis of real data has commenced.

J. Fyen
E.S. Husebye
F. Ringdal

Reference

Ringdal, F., E.S. Husebye and J. Fyen (1977): Earthquake detectability estimates for 478 globally distributed seismograph stations, Phys. Earth Planet. Inter., 15, P24-P32.

VI.5 Near-Field Wave Propagation Problems

The event detectability study outlined in Section VI.4 is essentially an analysis of P-wave amplitude distribution as a function of epicentral distance, although the results also depend on local station factors like the geological setting at the site, noise conditions, operational quality and so on. From an event discrimination point of view, we are also interested in strong phases in the near-field recordings, not only the excitation level of the traditionally studied P- and Rayleigh-waves. For example, an unresolved question is whether or not so-called Lg-waves propagate unhampered across prominent tectonic features like the Urals and Himalayas, and also what the relative significance of this phase is in the near-field range. In order to answer these and related questions, we have started a relatively comprehensive analysis of near-field earthquake and explosion recordings from seismographic stations in Eurasia in addition to our own NORSAR recordings. In the following we will present the observational data presently under consideration, the method of analysis and finally some comments on preliminary results.

WWSSN-station data base

Notwithstanding the many advantages of seismic tape recordings, on one account the analog WWSSN-records are superior, as they in a visual and compact form convey the essence of seismic recordings, namely, the relative energy distributions and the associated group velocities (or apparent group velocities). In this context we have collected, so far, about 320 copies of Eurasian WWSSN recordings at the U.K. seismological data library in Edinburgh. It is already now clear that this data base has to be greatly extended in order to obtain reliable multidimensional earthquake/explosion discriminants as we have to know in detail the group velocity interval for the energetic parts of seismic recordings for the largest possible ensemble of source-station combinations (for further details, see Section VI.6).

The first step in analysis of these records is to measure arrival times and maximum amplitudes of all prominent phases - wave trains for epicentral distances less than approx. 25°. In the second step of analysis we measure the group velocity interval associated with the most energetic wavetrains in the records, and also check the mode of propagation, that is, fundamental and higher modes of Love and Rayleigh waves. For this particular task the WWSSN-analysis will be complemented by very detailed analysis of digital NORSAR and SRO-records.

Preliminary results

Manual analysis of analog records is a rather time-consuming venture, so only preliminar results are available at present and are as follows:

- P-waves (P_g, P_b or P_n) are generally among the very strongest in the SP records. The most energetic phases here have in general velocities roughly linear with distance out to 20° in the bracket 7.0-7.5 km s^{-1} generally associated with P_b.
- S-waves and/or higher mode Love-Rayleigh waves have velocities around 4.5 km s^{-1} (Sn-waves), around 3.80 km s^{-1} (Li-waves) and 3.35-3.54 km s^{-1} (Lg1 and Lg2 waves). Sn, Li, Lg1 and Lg2 are now generally interpreted in terms of higher mode Love and Rayleigh waves, or as alternatives to the conventional Sn, Sb and Sg notations, for which the mode of propagation involves the uppermost part of the mantle. Specifically no low velocity layer below Moho is required for their explanation (e.g., see Knopoff et al, 1974; Mantovani et al, 1977; Panza and Calcagnile, 1975). We note in passing that initially Lg and Li waves conceptionally were associates with low velocity layers in the crust - Lg for shear waves in the granite (g) layer and Li in the basalt or intermediate (i) layer (Båth, 1962).
- Irrespective of source type, Sn (approx. 4.5 km s^{-1}) and fundamental mode Rayleigh waves besides occasional P-phases dominate the LP-records. Li is seldom seen, and Lg almost never.
- In Sp records Lg-waves are prominent together with various P phases. In case of explosive sources Lg-waves sometimes completely dominate the records with amplitudes slightly larger on the horizontal components. The most efficient transmission paths for Central Asian events appear to be westward towards Fennoscandia, whereas propagation is less efficient towards India, Pakistan and Iran. For earthquake records - usually exhibiting somewhat lower signal frequencies as compared to explosion sources - Lg-waves from our preliminary observations appear to be less prominent. Beyond 12-15° the Lg-waves decrease rapidly.

For very short distances ($\Delta < 5^{\circ}$) the SP-records are relatively 'messy', demonstrating the importance of scattering and mode conversion effects associated with crustal heterogeneities.

It is somewhat premature to speculate on the potential event discrimination power of the Lg-phase in a near-field context. What we know so far is that the observed Lg-excitations vary considerably with source type (preference to high-frequency radiation), and source-receiver paths. The relative attenuation efficiencies of tectonic barriers like the Urals and Himalayas as well as thick sedimentary basins are difficult to assess with our present data base. However, this can and will be done, given a sufficiently large data base. How to handle this kind of information in a discrimination context is the topic of the next section.

J. Fyen
E.S. Husebye

References

Båth, M. (1962): Channel waves in the earth's continental crust, Scientia, 56, 1-8.

Knopoff, L., F. Schwab, K. Nakanishi and F. Chang (1974): Evaluation of Lg as a discriminant among different continental crustal structures, Geophys. J.R. Astron. Soc., 39, 41-70.

Mantovani, E., F. Schwab, H. Liao and L. Knopoff (1977) Teleseismic Sn: a guided wave in the mantle, Geophys. J.R. Astron. Soc., 51, 709-726.

Panza, G.F., and G. Calcagnile (1975): Lg, Li and Rg from Rayleigh modes, Geophys. J.R. Astron. Soc., 40, 475-487.

VI.6 General Purpose Program for Seismic Discrimination

One of the current projects at NORSAR is to investigate the discrimination power of the Lg-phase for near-field observations. In this connection a general program has been completed which is based upon a feature-extraction procedure combined with classification statistics. The idea is to extract as few parameters as possible from the records and still preserve the main information (information pertaining to the second order statistics of the time series like the autocorrelation function or equivalently the power spectrum. The program is general in the sense that all the available information about an event is loaded into the computer and then the information carrying parameters is extracted and subsequently used for classification (for references, see Sandvin and Tjøstheim, 1978).

The input data to the program should be single parameters like the m_b-parameter for body waves, M_s-parameter for surface waves and/or some L_g-parameters considered to have a substantial discrimination potential. Combined with these parameters different time windows with amplitude registration from the seismogram starting from the onset of the chosen phase, may be incorporated in the input data file.

With registrations of the actual phases/wave trains for the same event but from different stations, the various time series may be combined into one multidimensional time series. In case of different frequency response of the seismometers, the traces should be filtered to remove the instrument response from the registrations. The feature extraction procedure consists of two steps. The first step is accomplished by fitting a multivariate autoregressive model of order P to the combined phase registrations described above.

$$\underline{x}(t) - A_1\underline{x}(t-1) \ldots - A_p\underline{x}(t-p) = \underline{z}(t)$$

Here $\underline{x}(t)$ denotes the vector registration at time t, A_i, i=1,2,...p are n x n matrices where n is the number of individual records, and $\underline{z}(t)$ an n-dimensional white noise vector.

The appropriate order p of the model should be determined from a criterion given by Akaike (1971). The fit of the model to the observations is evaluated by checking the whiteness of the residual process $\underline{z}(t)$. If the model is found appropriate, the second order statistics of the multi-dimensional time series as given by the individual spectra and the co-spectra are completely specified from the matrices A_i and the variance matrix V of the white noise process.

The second step of the feature extraction procedure is to combine the parameters contained in the matrices A_i with the single input parameters (m_b, M_s, etc.) from the different stations into a vector $\underline{Y}$ and then apply a principal component analysis to this vector. The idea in the principal component analysis of $\underline{Y}$ is to pick vectors $\underline{h}_i$, i=1,2,...,m in such a way that the main part of the information as expressed by the variation of $\underline{Y}$ is decomposed along a few of the vectors $\underline{h}_i$. The basis vector h_i are given by the eigenvalue problem:

$$R\,\underline{h}_i = \gamma_i \underline{h}_i$$

where R is the covariance matrix $E\{\underline{Y}\,\underline{Y}^T\}$. The estimation of the covariance matrix for earthquakes, R_{EQ} and for explosions R_{EX} requires a data base of presumed earthquakes and of presumed explosions.

Now for each event the estimated vector $\underline{Y}$ is decomposed along M_{EQ} principal vectors $h_{i_{EQ}}$ for the earthquake data base and along M_{EX} principal vectors $h_{i_{EX}}$ for the explosion data base with components

$$Z_{EQ}(i) = \underline{Y}^T \cdot \underline{h}_{i,EQ}, \qquad i = 1,2,\ldots, M_{EQ}$$

and

$$Z_{EX}(j) = \underline{Y}^T \cdot \underline{h}_{j,EX}, \qquad j = 1,2,\ldots, M_{EX}$$

respectively.

The components are finally combined into one vector

$$\underline{Z}^T = [Z_{EQ}(1),\ldots,Z_{EQ}(M_{EQ}),\ Z_{EX}(1),\ldots,Z_{EX}(M_{EQ})]$$

The vector $\underline{Z}$ is then regarded as a stochastic variable with distribution function F_{EQ} or F_{EX} depending on whether the event is an earthquake or an explosion. It is assumed that F_{EQ} and F_{EX} are the multivariate Gaussian distribution with the mean value and covariance matrix for each population determined from the earthquake data base and the explosion data base respectively. The discrimination is then accomplished by a classification procedure where the event is assigned to the population having the highest probability of $\underline{Z}$ occurring. As pointed out (Azen et al, 1975), the classification procedure is relatively robust to deviations from normality. Added flexibility to this particular discrimination is needed in order to handle missing observations and also changes in the number of reporting stations with changing source regions.

At present an extensive analysis of the Lg-phase from near-field (within 20^o) observations obtained from WWSSN is going on. It is concluded that the Lg-phase observations as well as those of Sn are evident from these readings and the amplitudes should be included in the input data to the program described above.

Finally, if the Lg-phase may turn out to be a potential discrimination parameter, SRO-recordings should be provided in order to apply the feature extraction procedure to that section of the records where the Lg-phase is found. 'Identical Classification Procedures' should be applied to different two-dimensional discriminants, like the well-established m_b:M_s criterion, to have the opportunity to give a precise comparison of the different discriminants.

O.A. Sandvin

References

Akaike, H. (1971): Autoregressive model fitting for control, Ann. Inst Stat. Math. 23, 163-180.

Azen, S.P., L. Breiman and W.S. Meisel (1975): Modem approaches to data analysis, Course notes. Technology Service Corporation, Santa Monica, California.

Panza, G.F., and G. Calcagnile (1974): Lg, Li and Rg from Rayleigh Modes, Geophys. J.R. Astron. Soc., 40, 475-487.

Robinson, E.A. (1967): Multichannel time series analysis with digital computer programs, Holden-Day, San Francisco.

Sandvin, O.A., and D. Tjøstheim (1978): Multivariate autoregressive representation of seismic P-wave signals with application to short-period discrimination, Bull. Seism. Soc. Amer., 68, 735-756.

Seismic Discrimination, 31 March 1978. Semiannual Technical Summary, M.I.T. Lincoln Laboratory, Cambridge, Mass.

VI.7 Do Geological Surface Features Have a Counterpart in the Deeper Part of the Lithosphere

Questions of the kind indicated in the heading of this section are frequently raised when efficiency of Lg-propagation along certain source-receiver paths are discussed. For example, mountain ranges like the Urals and Himalayas are intuitively associated with roots in the deeper lithosphere and thus act as barriers to Lg-propagation across such features. As regards the Himalayas there are, as also reported in a previous section, considerable observational evidence in support of the above hypothesis

In this context it may be appropriate to ask whether manifestations of less prominent tectonic activities like taphrogenesis have a counterpart in the lower lithosphere and thus affect the efficiency of Lg-propagation across such structures. As part of such an experiment we have tried to find out whether the Oslo graben has a seismic counterpart in the crust and upper mantle below the NORSAR array - the problem was mainly unsettled - in the Aki, Christoffersson and Husebye (ACH) (1977) travel time inversion experiment and this also applies to the amplitude modelling experiments by Haddon and Husebye (1978).

In order to answer the above question, we have modified the ACH-inversion techniques by imposing two types of restrictions on the parameter vector m:

- Some of the elements or blocks are zero, e.g., all m_i's within a particular layer are zero, which physically means that the layer represents homogeneous structures.
- Some of the elements are equalized, e.g., the blocks encompassed by the surface contours of the Oslo graben are made equal and thus constitute a <u>large</u> structural unit.

The above modified version of the ACH-inversion technique has been tested in the Oslo graben using the Haddon and Husebye time residual data base (more than 4000 observations). Relevant results are shown in Figs. VI.7.1 and VI.7.2 for which we have concluded that the surface graben contours have a seismic counterpart in the crust but probably not below Moho or at best it is very weakly represented here. This result is in good agreement with those derived from corresponding gravity observations as demonstrated by Husebye et al (1978).

The next step is, as mentioned above, to analyze proper observational data in order to check the propagation efficiency of high-frequency waves across a minor crustal tectonic feature.

A. Christoffersson, Dept. of Statistics,
Uppsala University
E.S. Husebye

References

Aki, K., A. Christoffersson and E.S. Husebye (1977): Determination of the three-dimensional seismic structure of the lithosphere, J. Geophys. Res., 82, 277-296.

Haddon, R.A.W., and E.S. Husebye (1978): Joint interpretation of P-wave time and amplitude anomalies in terms of lithospheric heterogeneities, Geophys. J.R. Astr. Soc., 55, 19-44.

Husebye, E.S., P.C. England and I.B. Ramberg (1978): The ideal-body concept in interpretation of the Oslo rift gravity data and their correlation with seismic observations, In: I.B. Ramberg & E.R. Neumann (Eds.), Tectonics and Geophysics of Continental Rifts, 313-327, D. Reidel Publ. Co., Dordrect, The Netherlands.

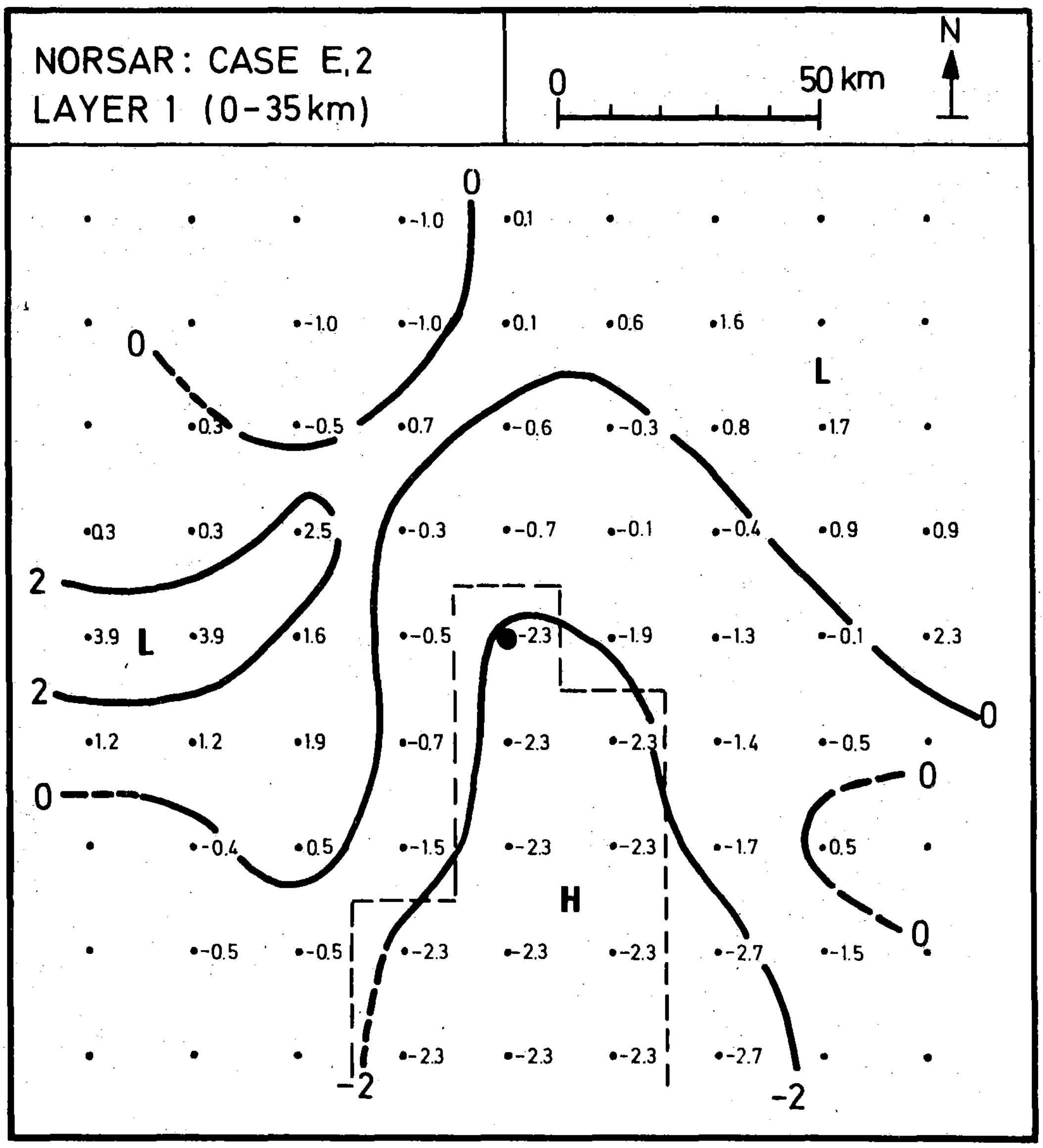

Fig. VI.7.1 a) Estimated seismic velocity anomalies in the crust of the NORSAR siting area. The Oslo graben contours are outlined and considered as one structural unit in the inversion experiment. A 3-layered standard earth model was used with Layer 2 removed or 'declared' homogeneous. Average layer velocity was 6.9 km s^{-1}, block size or horizontal extent of blocks is 20 x 20 km^2, and non-hit blocks are marked by a dot. High and low velocity areas are marked by the letter H and L respectively. For computational details, we refer to Aki et al (1977) and Christoffersson and Husebye (in preparation). We take these results to indicate that the surface contours of the Oslo graben have a seismic counterpart in the crust.

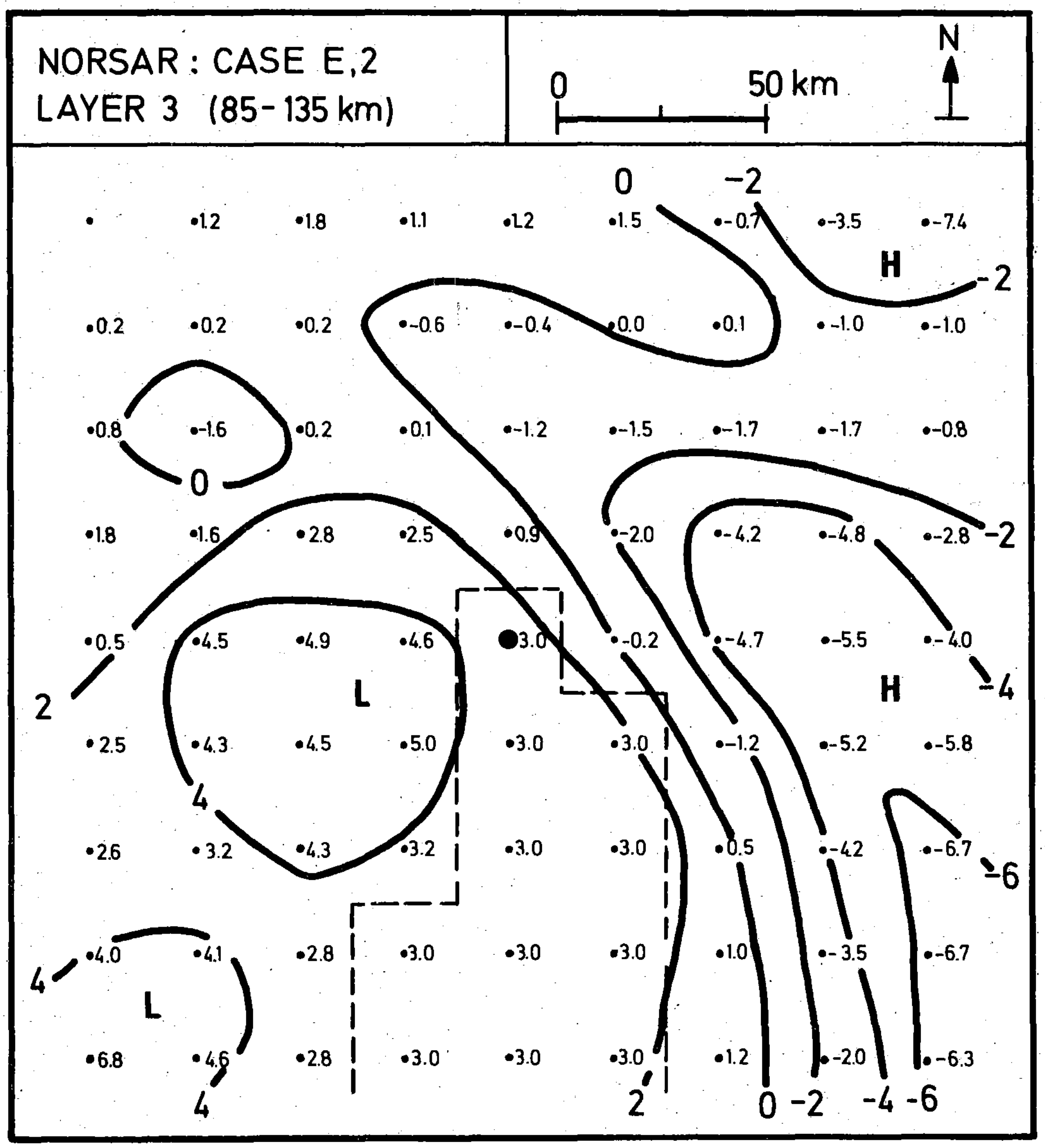

Fig. VI.7.2 These results plus estimated model fit parameters are taken to indicate that the graben imprints on the lower lithosphere are at best modest. Otherwise, caption as for Fig. VI.7.1.

VI.8 Description of and Preliminary Results from a Seismic Network for Microearthquake Studies in Tanzania

The African continent has until now been fairly poorly covered with seismic stations, and this applies in particular to Eastern Africa. In our capacity as seismological consultants in connection with the planning of a 1200 MW hydroelectric power plant in the Rufiji Basin in Tanzania, NTNF/NORSAR has recently completed the installation of a modern network of 6 short period seismometers in the area. The installation, which is called the Stiegler's Gorge Seismic Network (SGSN), has an aperture of about 50 km (see Fig. VI.8.1), and is located around 8°S, 38°E (see Table VI.8.1). This is about 1000 km from any previously known seismic station. The individual stations of the SGSN are powered by solar panels and the data are transmitted by radio telemetry to a Central Recording Station near the future dam site (see Fig. VI.8.1), where the analog data are passing a voting detector (presently 2 out of 3) and subsequently recorded on digital magnetic tapes whenever the detection threshold is exceeded. A memory buffer (sampling in retrospect) provides a few seconds of noise data preceding the event on each channel.

The SGSN has been installed for two main purposes: (1) to provide local seismicity data for phase II of the seismic risk analysis for the planned dam (Phase I has been completed), and (2) to provide seismological background data for the possibility of induced seismicity (in accordance with, e.g., recommendations from the UNESCO International Committee on Large Dams). It is obvious, moreover, that the network will be of considerable interest also from a more general seismological point of view, in particular for the study of the East African Rift System, including the Gregory Rift in whose extension the network is located. The planned operational period for the array is 2 years, although one hopes for an extension.

Preceding the installation of the network (completed in September 1978), a portable analog seismograph was operated sporadically for a few months, mainly for site surveys. Two things became obvious quite soon: (1) the local seismicity level is quite high, and some of this activity is very close to the dam site, (2) the ambient noise level is very low (seasonal variations are possible). As to the latter point, the portable seismograph could easily be operated at a magnification of 90 000 at 1 Hz, and an analog output from the permanent stations is usually kept at a magnification of about 120 000 at 1 Hz. This means that the RMS noise level at 1 Hz is not much above 1 nm.

Following the installation of the array, two timed explosions were fired near the dam site in order to provide an initial velocity model for the area. The results indicate significant velocity variations over the array (2 of the stations are on Basement, 4 are on Karroo), while on the average the data were best satisfied by a model with a P velocity of 5.0 km/s down to 4 km, followed by a layer with 5.9 km/s. So far only a few well-recorded events have been received and analyzed, one of which is presented in Fig. VI.8.2. The earthquake is located at a depth of 10 km about 4 km NE of the dam site (see Fig. VI.8.1), a point from which other events have been recorded as well. Most of the quakes seem to occur at depths between 10 and 20 km, and connected to a fault system (Tagalala) which runs from NW to SE very close to seismometer 2 and 3 (Fig. VI.8.1). Finally, an example of a teleseismically recorded earthquake is given in Fig. VI.8.3, showing an analog recording at one of the network stations of the disastrous Iran earthquake on 16 September 1978; M_s=7.3 measured at NORSAR.

The installation, operation and data analysis of the Stiegler's Gorge Seismic Network are funded by the Norwegian Agency for International Development.

H. Bungum

J. Fyen

Station	Lat.	Long.	Elev (m)
1	$7^{o}56.431'S$	$37^{o}50.445'E$	204
2	$7^{o}44.718'S$	$37^{o}53.189'E$	334
3	$7^{o}51.213'S$	$38^{o}\ 2.819'E$	162
4	$8^{o}\ 7.226'S$	$37^{o}50.791'E$	268
5	$7^{o}55.327'S$	$37^{o}35.577'E$	288
6	$7^{o}45.009'S$	$37^{o}39.516'E$	275

TABLE VI.8.1

Coordinates for the Stiegler's Gorge Seismic Network (SGSN)

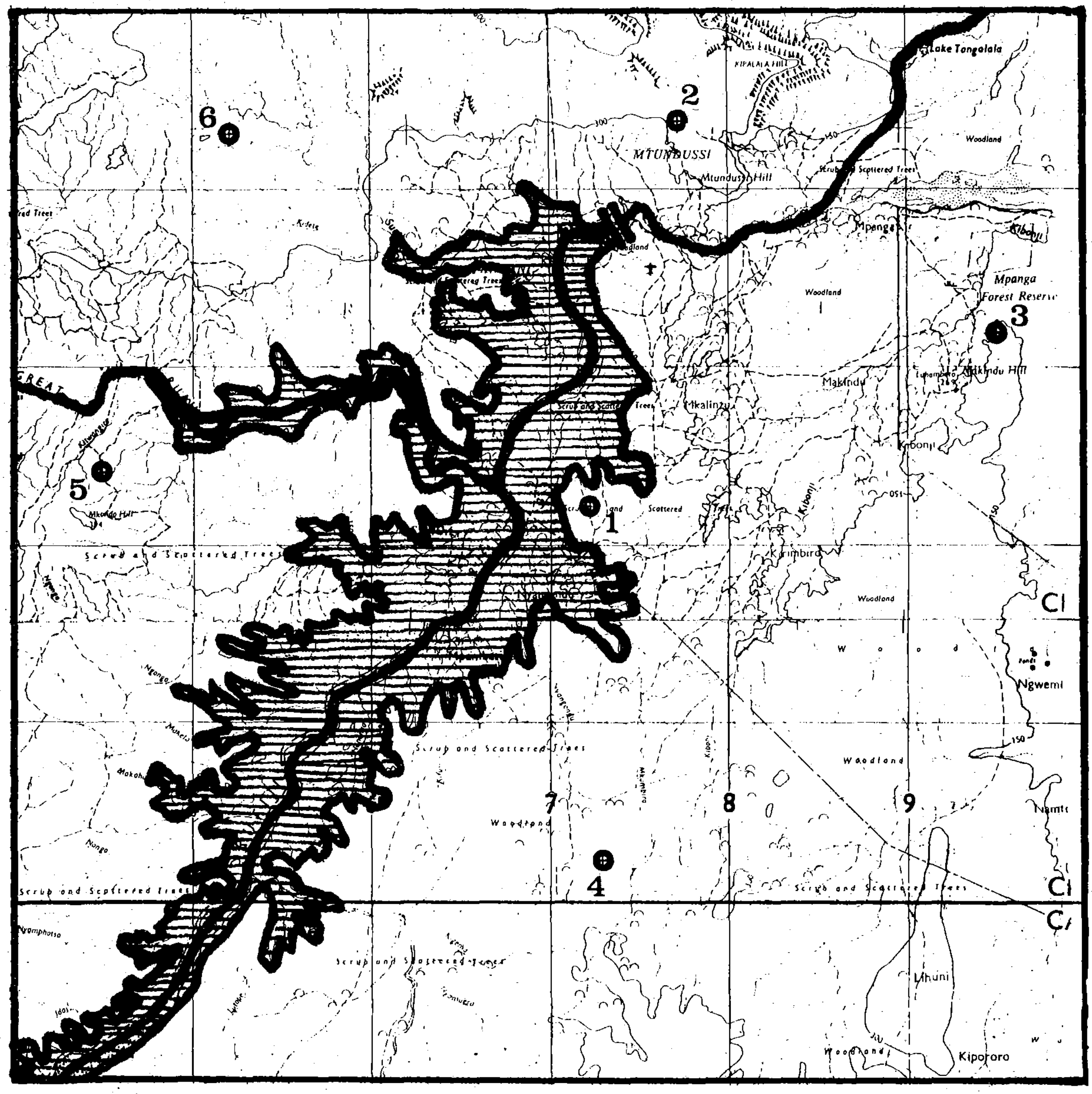

Fig. VI.8.1 Locations of the 6 stations of the Stiegler's Gorge Seismic Network (SGSN) in Tanzania. The Central Recording Station is situated just north of the dam site, close to seismometer No. 2. The water flows from SW to NE, and the hatched area is the future reservoir at a level of 150 m, which is 20-30 m below the planned maximum. The map covers 60 x 60 km.

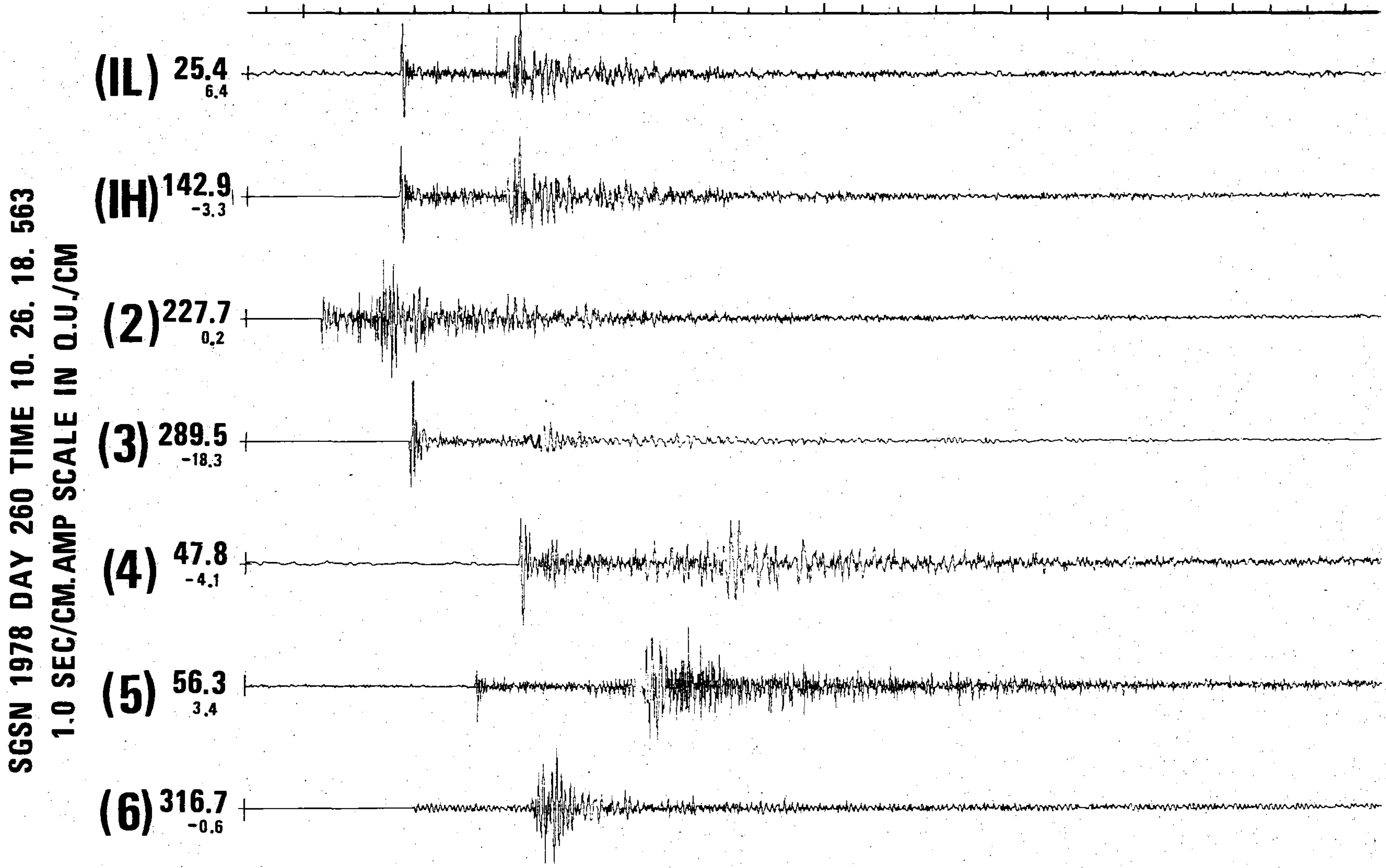

Fig. VI.8.2 A local earthquake on 17 September 1978 recorded by the Stiegler's Gorge Seismic Network. The time marks on the top are one second apart, and the first trace is a low-gain version of Station 1. The earthquake is located near Station 2 at 7°46.36'S, 37°52.34'E and at a depth of 10.1 km. Note especially the clear onsets and the changes in polarity.

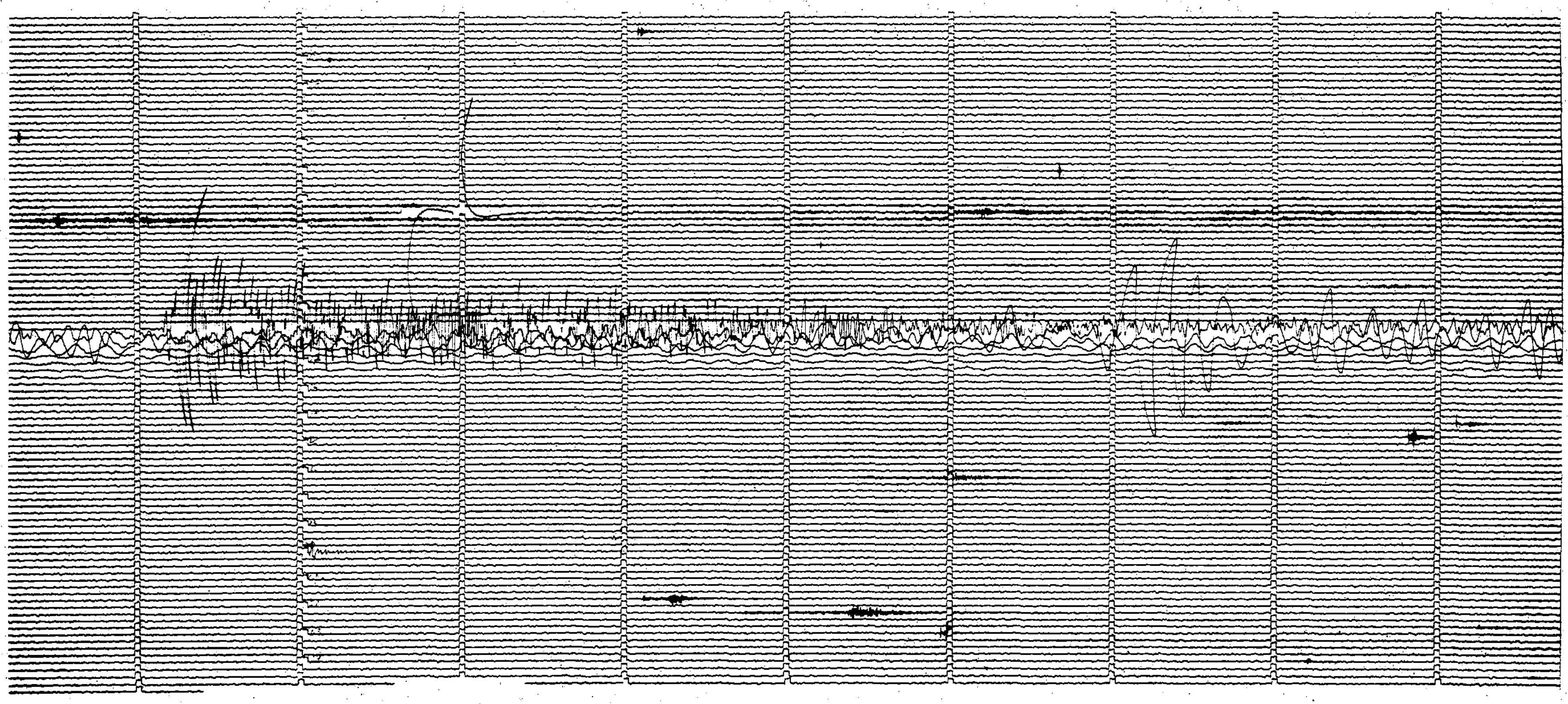

Fig. VI.8.3 Analog recording from Station 2 of the Stiegler's Gorge Seismic Network showing the disastrous Iran earthquake on 16 Sep 1978. Note especially the strong surface waves.

VI.9 The Seismicity of Svalbard

Our investigation of the seismicity of Svalbard has continued as outlined in the previous Semiannual Technical Summary (STS). Extensive and detailed analysis of the recorded data have been completed up to the end of May 1978, giving us almost 6 months altogether. The stations BBG, LYR and PRD have been in operation most of the time, the WWSSN station KBS has been in operation (and available to us through the University of Bergen) all of the time, and a new station SWE became operational in the beginning of May 1978.

Some figures on the detectability of the stations are given in Table VI.9.1, where it is seen that 1258 events have been reported altogether. 878 or about 70% of these are local events from Svalbard and vicinity (including the mid-Atlantic Ridge west of Svalbard), while the rest are teleseismic. With the exception of SWE (where there have been severe problems with local noise from the mines) we see from Table VI.9.1 that the teleseismic detectability is around 2 events/day for all stations, while it is LYR which is the best station so far as local events are concerned. A breakdown of the detectability statistics on a weekly basis is shown in Fig. VI.9.1, where we see that about 30-60 events have been detected every week. The figure also shows the division between teleseismic and local events, and the number in the latter group which have been located. Altogether 566 of the earthquakes have been located, which amounts to 64% of the local ones and 45% of the total number.

Since our report in the previous STS, two important improvements have been added to our location procedure. First, a crustal model for the area has been developed using our recordings of the signals from a profiling survey performed last summer by the University of Bergen (Prof. Sellevoll, personal communication) in cooperation with the University of Hamburg and the Polish Academy of Sciences. Our preliminary model derived from these data consists of layers with P velocities of 5.7, 6.7 and 8.2 km/s, starting at depths of 0, 16 and 32 km, respectively. The P to S velocity ratio is 1.80. The second improvement in our locations is connected to the location method itself. We have tried to use location programs such as HYPO71 (from USGS) but cannot obtain satisfactory convergence because of the poor station configuration with respect to the epicenter locations. A new method has therefore been developed which is based on the modified S-P method described in the previous STS, using the S-P location as a starting point and then refining the estimate using the absolute P times for the station for which reliable time corrections are available. Although the method in principle is similar to the one in HYPO71 (using the same information), it differs in the iterative procedure; our method has much stronger convergence properties for poor station configurations. The method is still being developed, and will be properly documented at a later stage.

An epicenter map from Svalbard using the new location method is given in Fig. VI.9.2, where only our most precise locations are plotted. 133 of our 566 located events are shown on this figure, and the number of phases used in each location ranges between 4 and 8 (S-P with no time correction counts as one phase). Reliable time corrections are available for at least one station for all of the events. The prominent feature is the now well-known Heerland earthquake zone, where any possible lineation still cannot be discerned, while it cannot be excluded either because of the precision of our epicenters. In comparing with the epicenter map in the previous STS, we see that the cluster of events now has been moved a little to the north-west, this is because of the new and imporved crustal model.

Besides the seismic activity along the mid-oceanic (Knipovich) ridge, there is one other feature in Fig. VI.9.2 which deserves attention, namely, the activity along the coast southwards from the WWSSN station KBS. Seven earthquakes are plotted in Fig. VI.9.2 along this (Forlandsundet) seismicity zone, which is reported here for the first time.

Some data on the measured local magnitudes are given in Fig. VI.9.3, which shows the incremental and cumulative distributions of magnitudes as measured from amplitudes. It is seen that the slope follows a value of b=1 down to a value of M=2.0, while the deviation below this value may be due to a combination of decreasing detectability, imprecise attenuation parameters in the magnitude formula, imprecise locations and the mixing of several epicentral areas in one distribution. It is important to notice, moreover, that our Svalbard magnitude scale has so far not been calibrated with respect to absolute level, this may cause a later shift of all the magnitudes by a constant value.

The Svalbard microearthquake network is operated by the Norwegian Polar Research Institute in cooperation with NTNF/NORSAR and the Russian mining trust Arktikugol.

H. Bungum
Y. Kristoffersen, Norwegian Polar Research Institute
B. Kr. Hokland

	BBG	PRD	LYR	SWE	KBS	Total
Teles.	291	291	229	18	310	380
-Daily	1.8	2.1	1.9	1.2	1.7	
Local	640	511	653	58	363	878
-Daily	3.8	3.8	5.4	4.0	2.1	
Sum	931	802	882	76	673	1258
-Daily	5.6	5.9	7.3	5.2	3.8	

TABLE VI.9.1

Detectability figures for the Svalbard microearthquake stations during the time period 8 Dec 1977 -31 May 1978. The daily averages are computed on the basis of the actual uptime for each station, which has been 95% for BBG, 77% for PRD, 67% for LYR, 8% for SWE (only part of May 1978) and 100% for the WWSSN station KBS. The locations of the stations are given in Fig. VI.9.2.

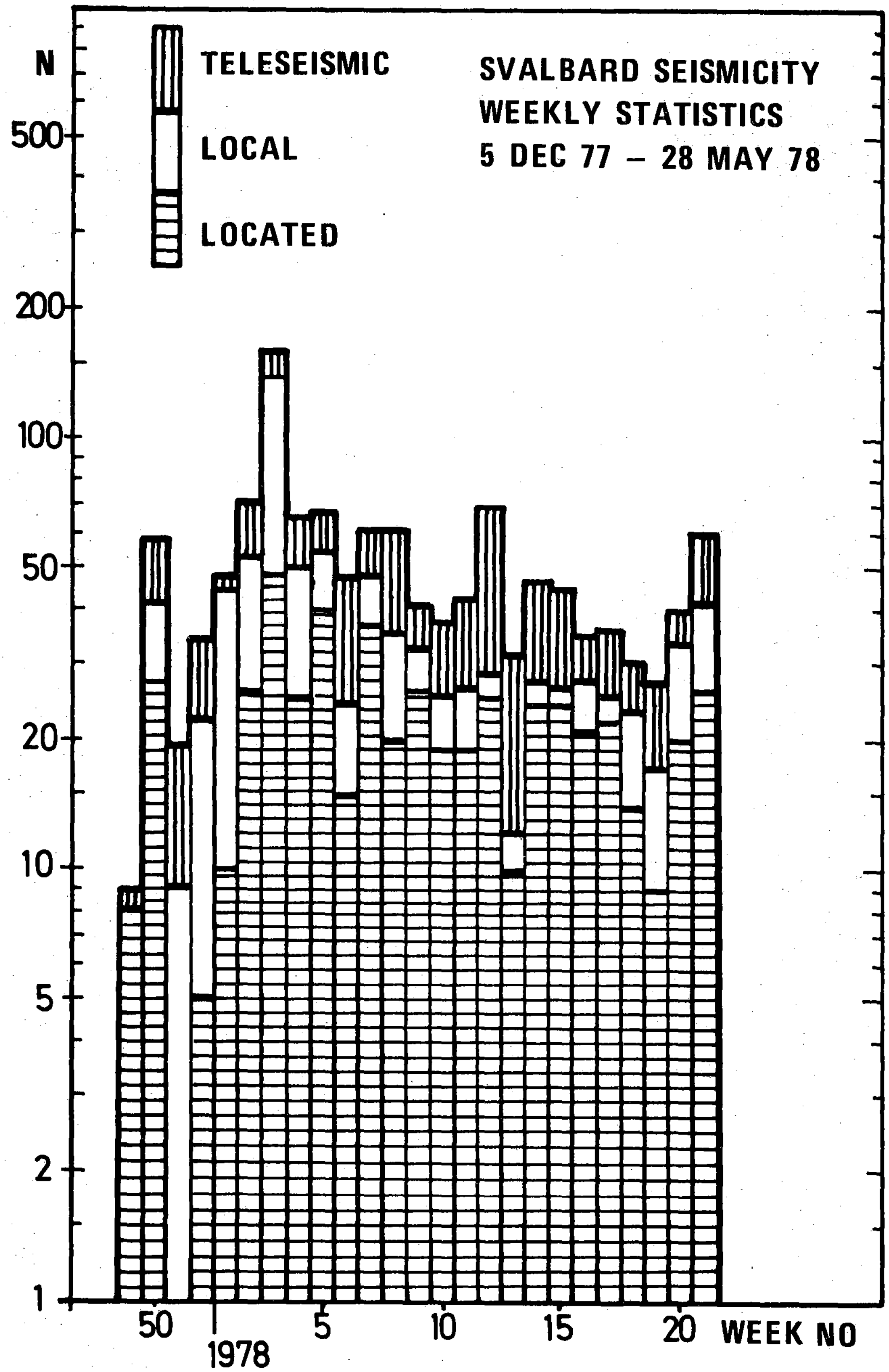

Fig. VI.9.1 Weekly breakdown of the number of earthquakes reported by the Svalbard microearthquake network in the 6 months between December 1977 and May 1978. The number of teleseismic, local and located (all local) events are shown separately. The peaks are due to swarms from the Knipovich Ridge and/or the Heerland earthquake zone (see Fig. VI.9.2).

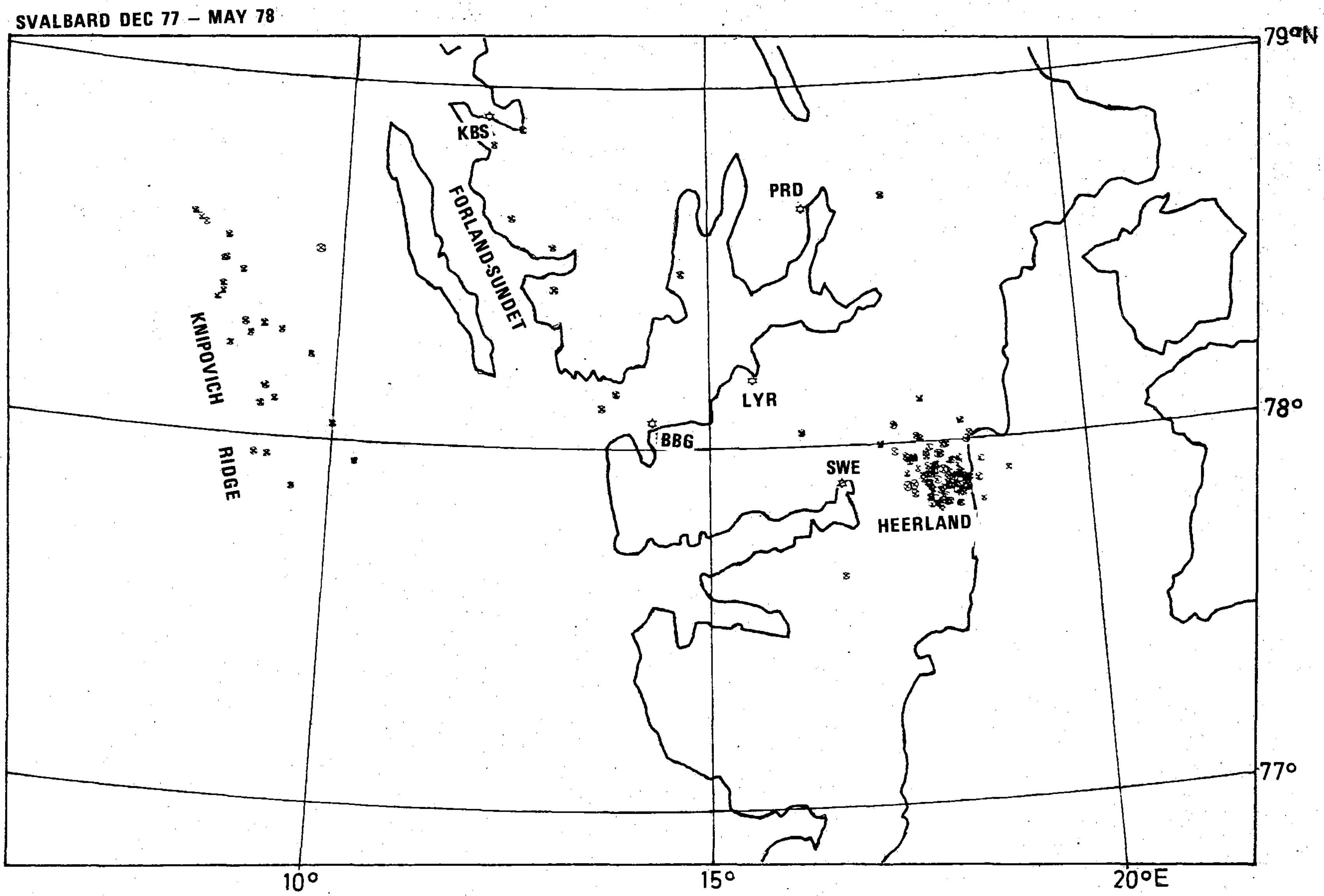

Fig. VI.9.2 Epicentral locations for the 133 most precisely located earthquakes from the Svalbard microearthquake network from December 1977 to May 1978.

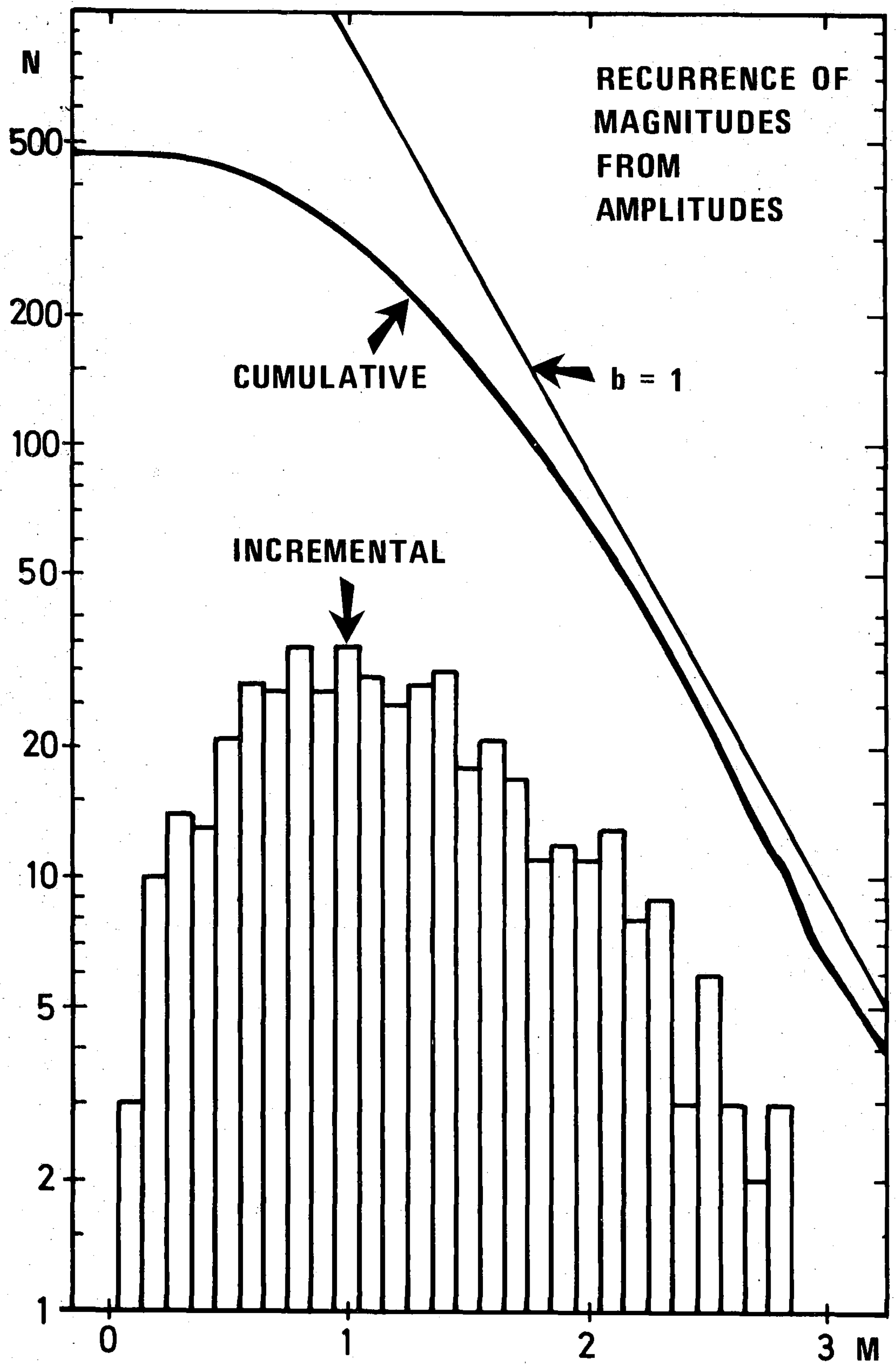

Fig. VI.9.3 Frequency-magnitude distribution for the located earthquakes in and around Svalbard, Dec 77 - May 78. The formula used is

$M=\log(A) - \alpha_1+\alpha_2\log\Delta+C$

where A is maximum amplitude, Δ is epicentral distance, α_1 and α_2 are parameters, and C is a constant.